Bound and continuum state β^- decay of bare atoms: Enhancement of decay rate and changes in β^- decay branching

Arkabrata Gupta, Chirashree Lahiri, and S. Sarkar*

Department of Physics, Indian Institute of Engineering Science and Technology (Formerly, Bengal Engineering and Science University), Shibpur, Howrah-711103, India

(Received 29 August 2018; revised manuscript received 20 September 2019; published 20 December 2019)

We calculated rates of β^- decay to both continuum and bound states separately for some fully ionized (bare) atoms in the mass range A $\approx$60–240. One of the motivations of this work is that the previous theoretical calculations were very old and/or informatically incomplete. Probably no theoretical study on this subject has been done in the last three decades. For the calculation, we have derived a framework from the usual β^- decay theory used by previous authors. Dependence of the calculated rates on the nuclear radius and neutral atom Q values have been examined. We have used the latest experimental data for nuclear and atomic observables, such as β^- decay Q values, ionization energy, neutral atom β^- decay branchings, and neutral atom half-lives. Results of β^- decay rates for decay to continuum and bound states and the enhancement factor due to the bound state decay for a number of nuclei have been tabulated and compared with the previously calculated values, if available. The effective rate or half-life calculated for a bare atom might be helpful to set a limit on the maximum enhancement due to bound state decay. Finally, β^- decay branching for a bare atom has been calculated. The changes in branching in a bare atom compared with that in a neutral atom and for the first time branching flip for a few cases have been obtained. The reason for this branching change has been understood in terms of Q values of the transitions in the neutral and bare atoms. Verification of this branching change or flip phenomenon in bare-atom decay might be of interest for future experiments.

DOI: 10.1103/PhysRevC.100.064313

I. INTRODUCTION

It is well known that the usual theory of β^- decay presumes that the decay of a neutron to proton is accompanied by the creation of an electron and an antineutrino in continuum states. However, in a stellar plasma where atoms get partially or fully ionized, this continuum decay is not the sole option. Nuclear β^- decay to the bound states of the ionized atom is another probable channel. Also, bare atoms have been produced terrestrially and β^- decays have been studied in storage-ring experiments. In 1947, Daudel *et al.* [1] first proposed the concept of bound state β decay. This suggests that a nucleus has a possibility to undergo β^- decay by creating an electron in a previously unoccupied atomic orbital instead of the continuum decay. It is important to understand that the bound state decay process does not occur subsequently from the β^- decay of an electron previously created in the continuum state, it is rather the direct creation of an electron in an atomic bound state accompanied by a monoenergetic antineutrino created in the free state carrying away the total decay energy. This process has been studied both theoretically as well as experimentally over the past seven decades.

In case of a neutral atom, available phase space for the creation of an electron in a vacant atomic orbital is very small and therefore the bound state decay is almost negligible compared with the contribution of the continuum decay. Contrarily, ionization of atoms may lead to drastic enhancement of bound state β decay probability due to the availability of more unoccupied atomic levels. In some previous theoretical works from the 1960s to 1980s, various groups studied the continuum and bound state β decay for neutron, tritium, [2] and fully ionized (bare) heavy atoms [3–5]. However, in most cases, previous theoretical works were based on very old data and/or were informatically incomplete. Simultaneously, the development of experimental techniques has served fruitfully to detect bound and continuum state β decay channels of fully ionized atoms. In 1992, Jung *et al.* observed the bound state β^- decay for the bare ^{163}Dy atom [6] by storing the fully ionized parent atom in a heavy-ion storage ring. In the same decade, Bosch *et al.* studied the bound state β^- decay for fully ionized ^{187}Re [7] which was helpful for the calibration of a ^{187}Re-^{187}Os galactic chronometer [8]. Further experiments with bare ^{207}Tl [9] showed the simultaneous measurement of bound and continuum state β^- decay. However, the authors mentioned this decay as a single β^- transition process to a particular daughter level with 100% branching [9], whereas the present data [10] suggest three available levels among which the total β^- decay is distributed.

In earlier studies, Takahashi and Yokoi [3,5] investigated β transition (bound state β^- decay and orbital electron capture) processes of some selected heavy nuclei suitable for *s*-process studies. However, in their work, they had not given separately the bound state decay rate of bare atoms. Furthermore, in

*ss@physics.iiests.ac.in

another work, Takahashi *et al.* [4] studied the β^- decay of some bare atoms for which bound state β^- decays produce significant enhancement in decay rates and proposed measurement in storage-ring experiments. However, they did not take into account the contribution of transitions to all possible energy levels of the daughter nucleus in total β^- decay rate enhancement. As an example, according to the present β^- decay data [10], there are six possible β^- transitions from the [117.59 keV, 6^+] state of ^{110}Ag to various states of ^{110}Cd, but they had mentioned the contribution of only one transition.

With the availability of modern day experimental β decay half-lives in terrestrial conditions for the neutral atom, experimental Q values for β^- decays and atomic physics inputs, it becomes inevitable to revisit some of the earlier works. Moreover, in a previous work, Takahashi and Yokoi [3] addressed a few nuclei in their "case studies," undergoing β^- transitions, as some of the essential turnabouts in s-process nucleosynthesis, where contributions from atoms with different states of ionization were considered. However, the explicit study of bound and continuum state β^- transitions of bare atoms for most of these nuclei remained unevaluated to date, both experimentally as well as theoretically.

In the present work, our aim is to study the β^- decay of some elements in the mass range $A \approx 60$–240, which might be of interest for future experimental evaluations using a storage ring. In particular, calculations of β^- decay rates to the continuum as well as bound states of these fully ionized atoms, where information for neutral atom experimental half-life and β^- decay branchings are terrestrially available, have been performed. Most importantly, the study of effective half-lives for bare atoms will be helpful to set a limit for the maximum enhancement in β^- decay rate due to the effect of bound state decay channels. Moreover, we have also discussed the effect of different nuclear structure and decay inputs (Q value, radius, etc.) over the bound to-continuum decay rate ratio. In addition, some interesting phenomena of changes in β^- decay branching for a number of bare atoms along with some notable change in branching (branching flip) for a few of them have been obtained. The branching flip is obtained for the first time.

The paper is organized as follows: Sec. II contains the methodology of our entire calculation for bound and continuum state β^- decay rates for bare atoms, as well as comparative half-life ($\log ft$) for neutral atoms. In Sec. III A we discuss our results for neutral atoms, whereas in Sec. III B results for the bare atoms are discussed. The phenomenon of change in β^- decay branching for bare atoms compared with that in neutral atoms is also discussed explicitly in Sec. III B. The conclusion of our work is described in Sec. IV. Finally, we present a table for the calculated β^- decay rates in Appendix A followed by a discussion of the choice of spin-parity for unconfirmed states of neutral atoms in Appendix B.

II. METHODOLOGY

In this work, we deal with the allowed and first-forbidden β^- transitions for neutral and fully ionized atoms. The contributions of higher-order forbidden transitions are negligible in the determination of the final β^- decay rate and thus we have not tabulated the contributions for the same.

The transition rates (in s^{-1}) for allowed (a), nonunique first-forbidden (nu), and unique first-forbidden (u) transitions are given by [3–5]

$$\begin{aligned}\lambda &= [(\ln 2)/f_0 t](f_m^*) \quad \text{for } m = \text{a, nu} \\ &= [(\ln 2)/f_1 t](f_m^*) \quad \text{for } m = \text{u}. \end{aligned} \tag{1}$$

Here t is the partial half-life of the specific parent-daughter energy-level combination for which a transition rate has to be calculated and f_m^* is the lepton phase volume part described in detail, below in this section. For allowed and nonunique first-forbidden β^- decay, the expression for the decay rate function $f_0(Z, W_0)$ can be simplified to [11,12]

$$f_0(Z, W_0) = \int_1^{W_0} \sqrt{(W^2-1)} W (W_0 - W)^2 F_0(Z, W) L_0 dW. \tag{2}$$

The certain combinations of electron radial wave functions evaluated at the nuclear radius R (in units of $\hbar/m_e c$) were first introduced by Konopinski and Uhlenbeck [12] as L_k. The value for $k = 0$ can be approximated as

$$L_0 = \frac{1 + \sqrt{1 - \alpha^2 Z^2}}{2}. \tag{3}$$

Here, α is the fine-structure constant. In the work of Behrens and Jänecke [13], the authors had taken a different form of L_0, which includes a slight dependence on the momentum. However, we find that the L_0 approximation adopted in our calculation is in good agreement with that from Ref. [13] within the energy window considered.

In Eq. (2), W is the total energy of the β^- particle for a $Z - 1 \to Z$ transition and $W_0 = Q_n/m_e c^2 + 1$ is the maximum energy available for the β^- particle. Here the mass difference between initial (parent) and final (daughter) states of neutral atoms are expressed as the decay Q value (Q_n in keV). The term $F_0(Z, W)$ is the Fermi function for allowed and nonunique transition, given by [12]

$$\begin{aligned} F_0(Z, W) = {} & \frac{4}{|\Gamma(1 + 2\sqrt{1 - \alpha^2 Z^2})|^2} \\ & \times (2R\sqrt{W^2 - 1})^{2(\sqrt{1-\alpha^2 Z^2}-1)} \exp\left[\frac{\pi \alpha Z W}{\sqrt{W^2 - 1}}\right] \\ & \times \left|\Gamma\left(\sqrt{1 - \alpha^2 Z^2} + i\frac{\alpha Z W}{\sqrt{W^2 - 1}}\right)\right|^2. \end{aligned} \tag{4}$$

Similarly, for the unique first-forbidden transition, the decay rate function $f_1(Z, W_0)$ has the form reduced from Refs. [11,12] and is given by

$$\begin{aligned} f_1(Z, W_0) = {} & \int_1^{W_0} \sqrt{(W^2 - 1)} W (W_0 - W)^2 F_0(Z, W) \\ & \times [(W_0 - W)^2 L_0 + 9 L_1] dW, \end{aligned} \tag{5}$$

with L_1 given by

$$L_1 = \frac{F_1(Z, W)}{F_0(Z, W)} \left(\frac{W^2 - 1}{9}\right) \frac{2 + \sqrt{4 - \alpha^2 Z^2}}{4}. \tag{6}$$

The term $F_1(Z,W)$ for a unique β^- transition is given by [12]

$$F_1(Z,W) = \frac{(4!)^2}{|\Gamma(1+2\sqrt{4-\alpha^2Z^2})|^2}(2R\sqrt{W^2-1})^{2(\sqrt{4-\alpha^2Z^2}-2)} \times \exp\left[\frac{\pi\alpha ZW}{\sqrt{W^2-1}}\right] \times\left|\Gamma\left(\sqrt{4-\alpha^2Z^2}+i\frac{\alpha ZW}{\sqrt{W^2-1}}\right)\right|^2. \quad (7)$$

Equations (2) and (5) are general forms of $f_0(Z,W_0)$ and $f_1(Z,W_0)$. For more precise calculation of the f factor, one should in principle include various corrections in the integrand of Eqs. (2) and (5). Corrections due to atomic physics effects, radiative correction, and finite nuclear size effects might be important for such studies. For fully ionized atoms, corrections due to atomic physics effects, such as imperfect overlap of initial and final atomic wave functions, exchange effects that comes from the antisymmetrization of the emitted electron with the atomic electrons [14], and screening of the nuclear charge due to the Coulomb field of the atomic electronic cloud are not needed. For neutral atom, the decay to the atomic bound state should be negligible [14]. Also, the screening and exchange corrections together cancel a large part of the overlap correction [15]. Furthermore, the nonorthogonality effect becomes rapidly smaller as Z increases [4]. Some of the corrections have positive sign and some of them have negative sign. So unless all the corrections are taken together, the treatment for corrections to f factor will not be consistent. Therefore we have neglected these contributions both for bare and neutral atoms. We have included the correction due to the extended charge distribution of the nucleus on the β^- spectrum. This correction is $\Lambda_k(Z,W) \rightarrow \Lambda_k[1+\Delta\Lambda_k(Z,W)]$, where the term Λ_k can be written in terms of L_k and $F_0(Z,W)$ as [11,12]

$$\Lambda_k(Z,W) = F_0(Z,W)L_{k-1}\left[\frac{(2k-1)!!}{(\sqrt{W^2-1})^{k-1}}\right]^2, \quad (8)$$

in such a way that it reduces to $[F_0(Z,W)L_0]$ and $[9F_0(Z,W)L_1/(W^2-1)]$ for $k=1$ and 2, respectively. The correction term is given by [11]

$$\Delta\Lambda_k(Z,W) = (Z-50)[-25\times10^{-4} - 4\times10^{-6}W(Z-50)] \quad \text{for } k=1, \quad Z>50, \\ = 0 \text{ for } k=1, \quad Z\leqslant 50, \\ = 0 \text{ for } k>1. \quad (9)$$

The screened energy of the emitted electron (W') enters through $\Delta\Lambda_k(Z,W')$, where $W' = W - V_0(Z)$. We calculated $V_0(Z)$, following Gove and Martin [11], using an expression from Garrett and Bhalla [16]. This correction to the integrand in Eqs. (2) and (5) has an effect in the fourth decimal place of the f factor, which is consistent with Ref. [17] discussed for allowed β^- decay. So we dropped W' and used W in the integrand.

Note that, in the present work, we used experimental quantities such as Q value, half-life, and branching, which have uncertainties even up to the first decimal place [10,18]. So, in our treatment we neglected the screening effect, too, for neutral atoms. Therefore, by using Eqs. (8) and (9) in the integrand of Eqs. (2) and (5) one can calculate the values for $f_0(Z,W_0)$ and $f_1(Z,W_0)$ incorporating only finite-size corrections.

In the work of Hayes *et al.* [19], the authors took a different form of the finite-size correction involving the charge density, which has a complicated radial dependency. However, we find that the results from the present calculation are in agreement with the available experimental data [10].

Furthermore, from the above expressions [Eqs. (4) and (7)], it is evident that the factors $F_0(Z,W)$ and $F_1(Z,W)$ depend on the radius, thereby making the terms f_0 and f_1 [Eqs. (2) and (5)] radius dependent. Thus, in our present study, we used various radius values from different phenomenological models and experiments to study their effects on the final ft values. To calculate ft values for a nucleus, we extracted the half-life t for individual transition to daughter levels using the latest β-decay branching information available in the literature [10].

The lepton phase volume f_m^* [5] for the continuum state β^- decay can thus be expressed as

$$f^*_{m=\text{a,nu}}(\text{continuum}) = \int_1^{W_c}\sqrt{(W^2-1)}W(W_c-W)^2F_0(Z,W)L_0dW, \quad (10)$$

$$f^*_{m=\text{u}}(\text{continuum}) = \int_1^{W_c}\sqrt{(W^2-1)}W(W_c-W)^2F_0(Z,W) \times[(W_c-W)^2L_0+9L_1]dW. \quad (11)$$

Here $W_c = Q_c/m_ec^2+1$ is the maximum energy available to the emitted β^- particle, and Q_c is given by

$$Q_c = Q_n - [B_n(Z+1) - B_n(Z)]. \quad (12)$$

The term $[B_n(Z+1)-B_n(Z)]$ denotes the difference of binding energies for bound electrons of the daughter and the parent atom. The experimental values for all the atomic data (binding energies or ionization potentials) are availed from Ref. [18].

Furthermore, for bound state β^- decay of the bare atom, f_m^* takes the form [5]

$$f^*_{m=\text{a,nu}}(\text{bound}) = \sum_x \sigma_x(\pi/2)[f_x \text{ or } g_x]^2b^2 \quad (\text{for } x = ns_{1/2}, np_{1/2}), \quad (13)$$

$$f^*_{m=\text{u}}(\text{bound}) = \sum_x \sigma_x(\pi/2)[f_x \text{ or } g_x]^2b^4 \quad (\text{for } x = ns_{1/2}, np_{1/2}) = \sum_x \sigma_x(\pi/2)[f_x \text{ or } g_x]^2b^2(9/R^2) \quad (\text{for } x = np_{3/2}, nd_{3/2}). \quad (14)$$

Here $[f_x \text{ or } g_x]$ is the larger component of electron radial wave function evaluated at the nuclear radius R of the daughter for the orbit x. $[f_x \text{ or } g_x]$ is obtained by solving Dirac radial wave equations using the Fortran subroutine RADIAL by Salvat *et al.*

[20]. In our case, σ_x is the vacancy of the orbit, chosen as unity, and b is equal to Q_b/m_ec^2 where

$$Q_b = Q_n - [B_n(Z+1) - B_n(Z)] - B_{\rm shell}(Z+1). \quad (15)$$

For example, in the case of a bare atom, if the emitted β^- particle gets absorbed in the atomic K shell, then the last term of Eq. (15) will be the ionization potential for the K electron denoted by $B_K(Z+1)$.

III. RESULTS AND DISCUSSION

In this work, we calculated β^--decay transition rates to bound and continuum states for a number of fully ionized atoms in the mass range $A \approx 60$–240. One of the motivations is that there is some evidence that earlier works were not equipped enough to address the entire β^--decay scenario. This might be due to the unavailability of information about all the energy levels participating in transition processes.

As an example, Takahashi *et al.* [4] considered transitions for allowed (a), first-forbidden nonunique (nu), and first-forbidden unique (u) decay of parent nuclei to a few energy levels of daughter nuclei. For instance, in the case of the ^{228}Ra nucleus, the authors tabulated the decay from the ground state of the parent $[E(\text{keV}),\ J^\pi] = [0.0, 0^+]$ nucleus to $[6.3, 1^-]$ and $[33.1, 1^+]$ states of the daughter nucleus ^{228}Ac. However, these two transitions cover only the 40% of the total β^- decay branching of neutral ^{228}Ra atom from the ground state. With the latest experimental data [10], we find that there are two more available states of ^{228}Ac where the rest of the β^- decay from the ground state of ^{228}Ra occurs. In this section, it will be shown that the contributions of these four states are extremely important to the determination of the effective enhancement of β^- transition rates of bare ^{228}Ra as well as to understand the phenomenon of branching flip, which was discussed in Sec. III B.

For simplicity, this section is subdivided into two parts: The first section involves the calculation of $\log ft$ for the neutral atom, a necessary ingredient for the calculation of β^- decay rate of the bare atom. In the next section, the β^- decay transition rates of bare atoms have been discussed with a detailed explanation of Table II. The dependence of these decay rates on different parameters is also examined in the same section. Finally, we show and discuss the change in individual level branchings in fully ionized atoms.

A. $\log ft$ calculation for neutral atoms

It is evident from Eqs. (1)–(9) that the calculation for $ft = f_0t$(or f_1t) is one of the essential components in the determination of the transition rate λ, which in turn depends on the radius R of the daughter nucleus. However, $\log ft$ data obtained from Ref. [10] cannot provide the information of the R dependence of $\log ft$. As the present theoretical modeling for bare atoms depends on the radius (see Sec. II), we find it more accurate to calculate $\log ft$ for neutral atoms for different choices of radii.

In Appendix A, we present a table for bound and continuum-state β^- decay rates for bare atoms along with the values of $\log ft$ for corresponding neutral atoms at different radii and compare our calculations with existing theoretical as well as experimental results (see the Supplemental Material [21] for details). As explained in Sec. II, we tabulated $\log ft$ values only for allowed (a), first-forbidden nonunique (nu), and first-forbidden unique (u) transitions.

Here, in Table II, R_1 is the phenomenological radius evaluated as $R_1 = 1.2A^{1/3}$ fm, whereas R_2 is the nuclear charge radius in fm [22] and R_3 is the half-density radius given by [11] $R_3 = (1.123A^{1/3} - 0.941A^{-1/3})$ fm. We calculated $\log ft$ values for R_1, R_2, and R_3 and compared them with the existing data [10]. In addition, we tabulated the available values from previous calculations of Takahashi *et al.* [4] in the same table.

One can see that the change in radius may cause a change in the $\log ft$ value mostly in the second decimal place. In the next section, we show the effect of these variations on the transition rates for bare atoms.

Furthermore, from Table II and the Supplemental Material [21], note that our calculation matches with the experimental $\log ft$ data [10] in most cases up to the first decimal place. The agreement of our result with experimental data [10] confirms the applicability of the methodology adopted in the present study.

B. Bound and continuum decay rates of bare atoms

In the ninth and the eleventh column of Table II of Appendix A, bound and continuum state β^- decay rates of bare atoms are presented, respectively.

It is observed that the dependence on radius affects the bound (λ_B) and the continuum state (λ_C) decay rates in first or second decimal places, and the ratio λ_B/λ_C remains almost unaffected up to the first decimal place for most of the examined cases.

Furthermore, from Table II (also see the Supplemental Material [21]), we find that the values for λ_B and λ_C from our calculation agree with those of the existing theoretical results [4] quite well. The possible reasons for the slight mismatch between our calculation and that from Takahashi *et al.* [4] are mainly due to (i) the effect of the nuclear radius, (ii) the adoption of present-day Q values (for all Q_n, Q_c, and Q_b), (iii) availability of present-day β^- decay branching of neutral atoms, and (iv) the choice of significant digits. Despite that, the overall success of our calculation in reproducing available λ_B and λ_C for bare atoms once again justifies the extension of the present calculation to previously unevaluated cases.

It can again be shown from Table II that, in a transition from the parent nucleus $^AX_{Z-1}$ to different energy levels of the daughter nucleus ^AX_Z, the ratio λ_B/λ_C for all transitions are not same, rather it decreases with increasing Q_n value. It can be understood from the expressions in Eqs. (10)–(15) where the factors $f^*_{\rm continuum}$ and $f^*_{\rm bound}$ depend on Q_c and Q_b, respectively, which are again derived from the neutral atom Q value Q_n. Due to different Q_n values for different transitions, λ_B/λ_C can be identified as a function of Q_n. For the sake of understanding, in Fig. 1, we plotted the ratio λ_B/λ_C versus Q_n for the nuclei ^{115}Cd, ^{123}Sn, ^{136}Cs, and ^{152}Eu. In each case, dependence on Q_n is observed which can be fit to the form

$$\frac{\lambda_B}{\lambda_C} = a(Q_n)^b, \quad (16)$$

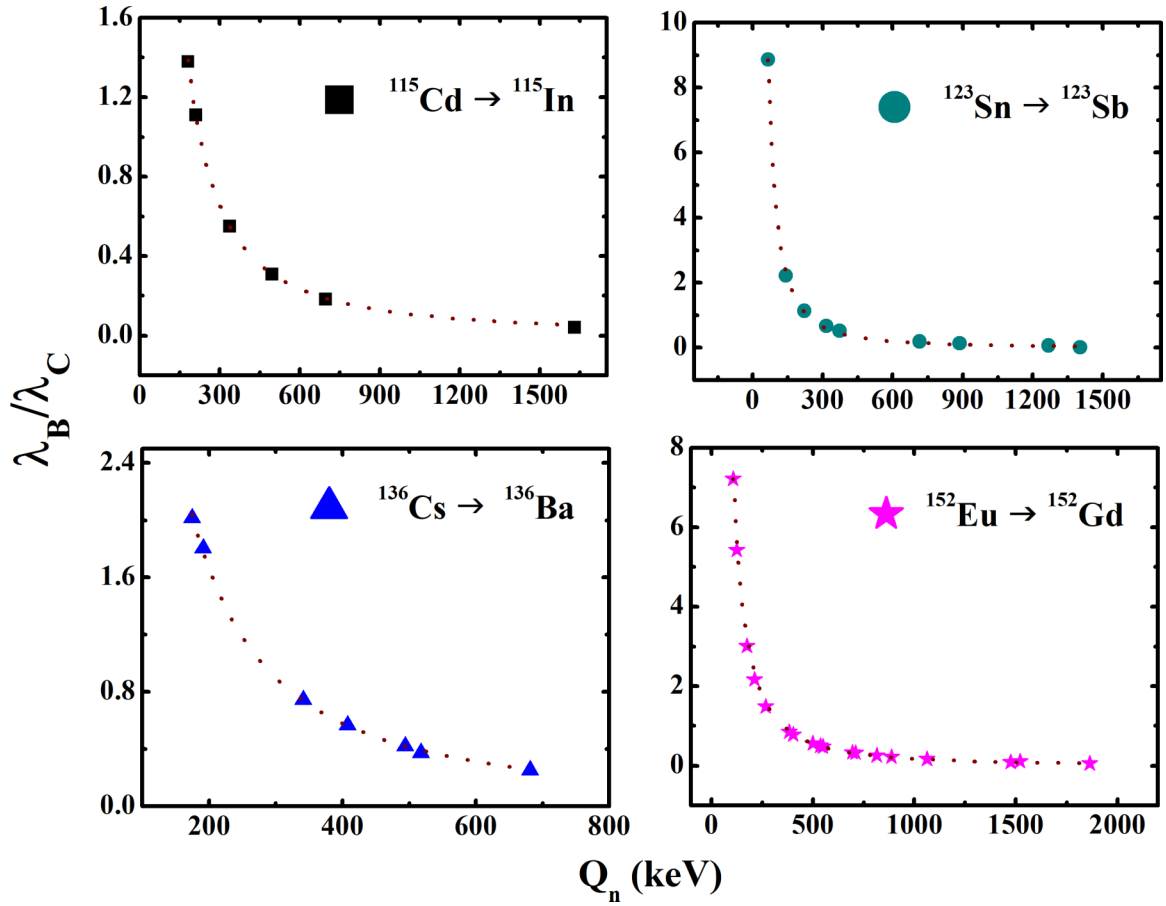

FIG. 1. Ratio of λ_B/λ_C vs the neutral atom Q value Q_n (in keV) for various β^- transitions (for the radius R_1). The dotted curves are obtained from fitting to Eq. (16). See text for details.

where a and b are the nucleus-dependent constants given in Table I.

Table I confirms that Eq. (16) is a characteristic feature of the λ_B/λ_C ratio of the bare atom with particular Z and A values. If there is a mistake in the calculation of f^* for λ_B or / and λ_C, then the ratio point will not fit to such a power law.

In the fourteenth column of Table II, the ratio of $\lambda_{\text{Bare}}(=\lambda_B+\lambda_C)/\lambda_{\text{Neutral}}$ (called here the rate enhancement factor) has been tabulated. It is evident from these values that there must be an enhancement in the decay rate for each transitions (i.e., $\lambda_{\text{Bare}}/\lambda_{\text{Neutral}} > 1$) because of the additional bound state decay channel.

In Fig. 2, the ratio of $\lambda_{\text{Bare}}/\lambda_{\text{Neutral}}$ for ^{110}Ag, ^{155}Eu, and ^{227}Ac have been shown. From the figure, it can be noted that rate enhancements (a) are different for different transitions of a particular nucleus, (b) are dependent on Q_n values: the lower the Q_n, the larger the enhancement. Moreover, this rate enhancement factor (c) also depends on Z and A of the atom; the larger the value of Z and/or A, the larger the enhancement.

Furthermore, in Table II, we have tabulated effective β^- decay half-lives for bare atoms and compared with those of neutral atoms. It should be noted that the neutral atom half-life given in the fifteenth column of the table is the total half-life corresponding to a, nu, and u types of β^- transitions only.

TABLE I. Parameters a and b for Eq. (16) for the radius R_1.

Parent → daughter	Parameter a	Parameter b
^{115}Cd → ^{115}In	3093.12 ± 317.17	−1.48 ± 0.02
^{123}Sn → ^{123}Sb	12 657.22 ± 1515.52	−1.73 ± 0.03
^{136}Cs → ^{136}Ba	5178.76 ± 654.04	−1.52 ± 0.02
^{152}Eu → ^{152}Gd	18 851.81 ± 1065.69	−1.68 ± 0.01

1. Transition details: Case studies

The dependence of the rate-enhancement factor on Q_n causes a change in β^- branching for the bare atom. In the bare atom, branchings similar to the neutral atom can only be achieved if the factor $\lambda_{\text{Bare}}/\lambda_{\text{Neutral}}$ remains constant with Q_n, which is obviously not the case (Fig. 2). In other words, this change can be understood to be an outcome of the nonuniformity of the λ_B/λ_C ratio with Q_n. It is observed that the continuum decay rate for bare atom decreases with respect to that for the neutral atom (i.e., $\lambda_C < \lambda_{\text{Neutral}}$) due to the reduction of the continuum Q value [$Q_c < Q_n$, Eq. (12)]. Furthermore, from Fig. 1, it is clear that, with the decrease in the Q_n value, λ_B dominates more over λ_C and hence the effective decay rate of the bare atom $\lambda_{\text{Bare}} = \lambda_B + \lambda_C$ does not follow the same branching as that of the neutral atom.

TABLE II. $\log f_0 t\,(f_1 t)$ values, bound and continuum state β^- decay rates (bare atom), comparison between neutral atom and bare atom β^- decay rates for different choices of radii compared with the results of previous theoretical work and experimental data.

Transition details				Radius	$\log f_0\,(\log f_1)$ calculations			Bare atom decay rates						Half-life	
					$\log f_0\,(\log f_1)$	$\log f_0 t\,(\log f_1 t)$		λ_B (s^{-1})		λ_C (s^{-1})					
Neutral				(fm)	Present	Present	Previous	Present	Previous	Present	Previous	λ_B/λ_C	$\lambda_{\text{Bare}}/\lambda_{\text{Neutral}}$	Neutral	Bare
Atom				R_1	(for R_1)	(for R_1)		(for R_1)		(for R_1)		(for R_1)	(for R_1)		(for R_1)
Branching	Parent → daughter		Q_n	R_2	(for R_2)	(for R_2)	Ref. [4]	(for R_2)		(for R_2)		(for R_2)	(for R_2)		(for R_2)
Ref. [10]	[E (keV), J^Π]	Type	(keV)	R_3	(for R_3)	(for R_3)	Ref. [10]	(for R_3)	Ref. [4]	(for R_3)	Ref. [4]	(for R_3)	(for R_3)		(for R_3)
	^{95}Nb → ^{95}Mo			5.475	2.2274	9.216		4.20×10^{-9}		6.89×10^{-8}		6.10×10^{-2}	1.03×10^{0}		
	[234.7, $\frac{1}{2}^-$] [0.0, $\frac{5}{2}^+$]	u	1160.300	4.363	2.2350	9.224	9.20	4.22×10^{-9}		6.89×10^{-8}		6.13×10^{-2}	1.03×10^{0}		
				4.918	2.2297	9.219		4.23×10^{-9}		6.88×10^{-8}		6.15×10^{-2}	1.03×10^{0}		
	^{95}Nb → ^{95}Mo			5.475	1.2432	8.357		3.92×10^{-9}		5.21×10^{-8}		7.53×10^{-2}	1.05×10^{0}		
	[234.7, $\frac{1}{2}^-$] [204.1, $\frac{3}{2}^+$]	nu	956.200	4.363	1.2533	8.367	8.4	3.92×10^{-9}		5.21×10^{-8}		7.53×10^{-2}	1.05×10^{0}		
				4.918	1.2463	8.360		3.95×10^{-9}		5.21×10^{-8}		7.58×10^{-2}	1.05×10^{0}		
	^{95}Nb → ^{95}Mo			5.475	−0.1873	8.455		5.02×10^{-10}		1.50×10^{-9}		3.36×10^{-1}	1.27×10^{0}		61.16 d
	[234.7, $\frac{1}{2}^-$] [786.2, $\frac{1}{2}^+$]	nu	374.100	4.363	−0.1772	8.466	8.4	5.01×10^{-10}		1.49×10^{-9}		3.36×10^{-1}	1.26×10^{0}	63.65 d	61.19 d
Fig. 6(a)				4.918	−0.1842	8.459		5.05×10^{-10}		1.49×10^{-9}		3.38×10^{-1}	1.26×10^{0}		61.18 d
	^{95}Nb → ^{95}Mo			5.475	−0.3258	10.600		2.99×10^{-12}		7.75×10^{-12}		3.86×10^{-1}	1.31×10^{0}		
	[234.7, $\frac{1}{2}^-$] [820.6, $\frac{3}{2}^+$]	nu	339.700	4.363	−0.3157	10.610	10.6	3.00×10^{-12}		7.74×10^{-12}		3.87×10^{-1}	1.31×10^{0}		
				4.918	−0.3227	10.603		3.01×10^{-12}		7.75×10^{-12}		3.89×10^{-1}	1.31×10^{0}		
	^{95}Nb → ^{95}Mo			5.475	−1.7577	10.622		4.19×10^{-13}		2.48×10^{-13}		1.69×10^{0}	2.31×10^{0}		
	[234.7, $\frac{1}{2}^-$] [1039.3, $\frac{1}{2}^+$]	nu	121.000	4.363	−1.7476	10.632	$\geqslant$10.3	4.19×10^{-13}		2.43×10^{-13}		1.73×10^{0}	2.29×10^{0}		
				4.918	−1.7546	10.625		4.22×10^{-13}		2.47×10^{-13}		1.71×10^{0}	2.31×10^{0}		
	^{110}Ag → ^{110}Cd			5.750	0.4463	8.285		2.56×10^{-9}		9.59×10^{-9}		2.67×10^{-1}	1.21×10^{0}		
	[117.59, 6^+] [2479.9, 6^+]	a	530.590	4.577	0.4586	8.297	8.277	2.58×10^{-9}		9.60×10^{-9}		2.68×10^{-1}	1.21×10^{0}		
				5.184	0.4541	8.293		2.55×10^{-9}		9.59×10^{-9}		2.66×10^{-1}	1.21×10^{0}		
	^{110}Ag → ^{110}Cd			5.750	0.2691	10.816		6.00×10^{-12}		1.86×10^{-11}		3.23×10^{-1}	1.26×10^{0}		
	[117.59, 6^+] [2539.7, 5^-]	nu	470.790	4.577	0.2814	10.830	10.81	6.00×10^{-12}		1.85×10^{-11}		3.24×10^{-1}	1.25×10^{0}		
				5.184	0.2770	10.826		5.95×10^{-12}		1.85×10^{-11}		3.21×10^{-1}	1.25×10^{0}		
	^{110}Ag → ^{110}Cd			5.750	−0.1586	10.619		5.39×10^{-12}		1.08×10^{-11}		5.02×10^{-1}	1.40×10^{0}		
	[117.59, 6^+] [2659.9, 5^-]	nu	350.590	4.577	−0.1464	10.632	10.61	5.40×10^{-12}		1.07×10^{-11}		5.03×10^{-1}	1.40×10^{0}		76.90 d
Fig. 6(b)				5.184	−0.1508	10.627		5.37×10^{-12}		1.08×10^{-11}		4.99×10^{-1}	1.39×10^{0}	0.69 yr	76.83 d
	^{110}Ag → ^{110}Cd			5.750	−1.1847	9.784		9.52×10^{-12}		6.38×10^{-12}		1.49×10^{0}	2.13×10^{0}		76.98 d
	[117.59, 6^+] [2842.6, $(5)^-$]	nu	167.890	4.577	−1.1724	9.796	9.773	9.56×10^{-12}		6.43×10^{-12}		1.49×10^{0}	2.15×10^{0}		
				5.184	−1.1768	9.792		9.48×10^{-12}		6.38×10^{-12}		1.49×10^{0}	2.13×10^{0}		
	^{110}Ag → ^{110}Cd			5.750	−1.4943	8.239		2.24×10^{-10}		1.08×10^{-10}		2.07×10^{0}	2.59×10^{0}		
	[117.59, 6^+] [2876.8, 6^+]	a	133.690	4.577	−1.4820	8.251	8.228	2.25×10^{-10}		1.05×10^{-10}		2.14×10^{0}	2.58×10^{0}		
				5.184	−1.4865	8.247		2.23×10^{-10}		1.06×10^{-10}		2.11×10^{0}	2.57×10^{0}		

^{110}Ag → ^{110}Cd			5.750	−2.1235	5.374	5.37	7.54×10^{-8}	7.8×10^{-8}	1.64×10^{-8}	1.7×10^{-8}	4.587×10^{0}	4.17×10^{0}	
[117.59, 6^+] [2926.7, 5^+]	a	83.790	4.577	−2.1112	5.387	5.365	7.55 × 10^{-8}		1.64 × 10^{-8}		4.60 × 10^{0}	4.17 × 10^{0}	
			5.184	−2.1156	5.382		7.51 × 10^{-8}		1.64 × 10^{-8}		4.57 × 10^{0}	4.15 × 10^{0}	
^{115}Cd → ^{115}In			5.836	2.2569	8.856		6.72 × 10^{-9}		1.71 × 10^{-7}		3.93 × 10^{-2}	1.02 × 10^{0}	
[181.0, $\frac{11}{2}^-$] [0.0, $\frac{9}{2}^+$]	nu	1629.700	4.616	2.2698	8.868	8.8	6.78 × 10^{-9}		1.72 × 10^{-7}		3.95 × 10^{-2}	1.02 × 10^{0}	
			5.268	2.2609	8.860		6.78 × 10^{-9}		1.71 × 10^{-7}		3.96 × 10^{-2}	1.02 × 10^{0}	
^{115}Cd → ^{115}In			5.836	1.1738	9.529		5.32 × 10^{-10}		2.89 × 10^{-9}		1.84 × 10^{-1}	1.12 × 10^{0}	
[181.0, $\frac{11}{2}^-$] [933.8, $\frac{7}{2}^+$]	u	695.900	4.616	1.1832	9.538	≈9.5	5.40 × 10^{-10}		2.89 × 10^{-9}		1.87 × 10^{-1}	1.12 × 10^{0}	
			5.268	1.1767	9.532		5.37 × 10^{-10}		2.89 × 10^{-9}		1.86 × 10^{-1}	1.12 × 10^{0}	
^{115}Cd → ^{115}In			5.836	0.3710	10.178		3.16 × 10^{-11}		1.03 × 10^{-10}		3.08 × 10^{-1}	1.24 × 10^{0}	
[181.0, $\frac{11}{2}^-$] [1132.6, $\frac{11}{2}^+$]	nu	497.100	4.616	0.3838	10.191	≈10.2	3.18 × 10^{-11}		1.03 × 10^{-10}		3.10 × 10^{-1}	1.24 × 10^{0}	
			5.268	0.3750	10.182		3.18 × 10^{-11}		1.03 × 10^{-10}		3.11 × 10^{-1}	1.24 × 10^{0}	
^{115}Cd → ^{115}In			5.836	−0.1840	8.447		8.23 × 10^{-10}		1.50 × 10^{-9}		5.50 × 10^{-1}	1.43 × 10^{0}	43.38 d
[181.0, $\frac{11}{2}^-$] [1290.6, $\frac{13}{2}^+$]	nu	339.100	4.616	−0.1712	8.460	≈8.4	8.28 × 10^{-10}		1.50 × 10^{-9}		5.53 × 10^{-1}	1.43 × 10^{0}	44.56 d 43.26 d
			5.268	−0.1800	8.451		8.29 × 10^{-10}		1.50 × 10^{-9}		5.54 × 10^{-1}	1.44 × 10^{0}	43.36 d
^{115}Cd → ^{115}In			5.836	−0.8471	8.261		5.27 × 10^{-10}		4.75 × 10^{-10}		1.11 × 10^{0}	1.86 × 10^{0}	
[181.0, $\frac{11}{2}^-$] [1418.3, $(\frac{9}{2})^+$]	nu	211.400	4.616	−0.8343	8.274	≈8.2	5.30 × 10^{-10}		4.76 × 10^{-10}		1.12 × 10^{0}	1.86 × 10^{0}	
			5.268	−0.8431	8.265		5.31 × 10^{-10}		4.78 × 10^{-10}		1.11 × 10^{0}	1.87 × 10^{0}	
^{115}Cd → ^{115}In			5.836	−1.0626	9.222		4.36 × 10^{-11}		3.16 × 10^{-11}		1.38 × 10^{0}	2.09 × 10^{0}	
[181.0, $\frac{11}{2}^-$] [1448.8, $\frac{9}{2}^+$]	nu	180.900	4.616	−1.0498	9.235	≈9.2	4.38 × 10^{-11}		3.15 × 10^{-11}		1.39 × 10^{0}	2.09 × 10^{0}	
			5.268	−1.0586	9.226		4.39 × 10^{-11}		3.13 × 10^{-11}		1.40 × 10^{0}	2.09 × 10^{0}	
^{115}Cd → ^{115}In			5.836	−1.3775	10.363		2.10 × 10^{-12}		1.05 × 10^{-12}		2.00 × 10^{0}	2.50 × 10^{0}	
[181.0, $\frac{11}{2}^-$] [1486.1, $\frac{9}{2}^+$]	nu	143.600	4.616	−1.3647	10.376	≈10.3	2.11 × 10^{-12}		1.05 × 10^{-12}		2.01 × 10^{0}	2.51 × 10^{0}	
			5.268	−1.3735	10.367		2.11 × 10^{-12}		1.07 × 10^{-12}		1.97 × 10^{0}	2.53 × 10^{0}	
^{123}Sn → ^{123}Sb			5.968	2.8398	9.890		4.31 × 10^{-9}		5.98 × 10^{-8}		7.22 × 10^{-2}	1.04 × 10^{0}	
[0.0, $\frac{11}{2}^-$] [0.0, $\frac{7}{2}^+$]	u	1403.600	4.688	2.8504	9.901	9.876	4.37 × 10^{-9}		5.97 × 10^{-8}		7.32 × 10^{-2}	1.04 × 10^{0}	
			5.396	2.8431	9.894		4.34 × 10^{-9}		5.96 × 10^{-8}		7.28 × 10^{-2}	1.04 × 10^{0}	
^{123}Sn → ^{123}Sb			5.968	−0.0045	10.552		9.32 × 10^{-12}		1.79 × 10^{-11}		5.19 × 10^{-1}	1.42 × 10^{0}	
[0.0, $\frac{11}{2}^-$] [1030.2, $\frac{9}{2}^+$]	nu	373.400	4.688	0.0094	10.566	10.54	9.37 × 10^{-12}		1.79 × 10^{-11}		5.23 × 10^{-1}	1.42 × 10^{0}	
			5.396	−0.0002	10.556		9.38 × 10^{-12}		1.79 × 10^{-11}		5.23 × 10^{-1}	1.42 × 10^{0}	

Fig. 6(c)

(Continued.)

Transition details				Radius	$\log f_0$ ($\log f_1$)	$\log f_0 t$ ($\log f_1 t$)		Bare atom decay rates						Half-life	
								λ_B (s^{-1})		λ_C (s^{-1})					
Neutral Atom Branching Ref. [10]	Parent → daughter [E (keV), J^Π]	Type	Q_n (keV)	(fm) R_1 R_2 R_3	Present (for R_1) (for R_2) (for R_3)	Present (for R_1) (for R_2) (for R_3)	Previous Ref. [4] Ref. [10]	Present (for R_1) (for R_2) (for R_3)	Previous Ref. [4]	Present (for R_1) (for R_2) (for R_3)	Previous Ref. [4]	λ_B/λ_C (for R_1) (for R_2) (for R_3)	$\lambda_{Bare}/\lambda_{Neutral}$ (for R_1) (for R_2) (for R_3)	Neutral	Bare (for R_1) (for R_2) (for R_3)
	^{123}Sn → ^{123}Sb			5.968	−0.2488	9.020		2.31×10^{-10}		3.44×10^{-10}		6.72×10^{-1}	1.54×10^{0}		
	[0.0, $\frac{11}{2}^-$] [1088.7, $(\frac{9}{2})^+$]	nu	314.900	4.688	−0.2349	9.035	9.01	2.31×10^{-10}		3.43×10^{-10}		6.75×10^{-1}	1.54×10^{0}		
				5.396	−0.2445	9.025		2.32×10^{-10}		3.43×10^{-10}		6.76×10^{-1}	1.54×10^{0}		
	^{123}Sn → ^{123}Sb			5.968	−0.7360	10.969		1.37×10^{-12}		1.21×10^{-12}		1.13×10^{0}	1.89×10^{0}		
	[0.0, $\frac{11}{2}^-$] [1181.3, $(\frac{9}{2})^+$]	nu	222.300	4.688	−0.7221	10.983	10.96	1.38×10^{-12}		1.24×10^{-12}		1.11×10^{0}	1.92×10^{0}		
				5.396	−0.7317	10.974		1.38×10^{-12}		1.19×10^{-12}		1.16×10^{0}	1.88×10^{0}		124.03 d
Fig. 6(d)	^{123}Sn → ^{123}Sb			5.968	−1.1233	10.582		[a]		[a]		[a]	[a]	129.20 d	124.01 d
	[0.0, $\frac{11}{2}^-$] [1181.3, $(\frac{7}{2})^+$]	u	222.300	4.688	−1.1146	10.591	10.96								124.26 d
				5.396	−1.1206	10.585									
	^{123}Sn → ^{123}Sb			5.968	−1.3441	11.558		1.62×10^{-13}		7.29×10^{-14}		2.22×10^{0}	2.70×10^{0}		
	[0.0, $\frac{11}{2}^-$] [1260.9, $(\frac{9}{2})^+$]	nu	142.700	4.688	−1.3302	11.572	11.55	1.63×10^{-13}		7.24×10^{-14}		2.24×10^{0}	2.70×10^{0}		
				5.396	−1.3398	11.562		1.63×10^{-13}		7.22×10^{-14}		2.26×10^{0}	2.70×10^{0}		
	^{123}Sn → ^{123}Sb			5.968	−1.9211	10.981		[a]		[a]		[a]	[a]		
	[0.0, $\frac{11}{2}^-$] [1260.9, $(\frac{7}{2})^+$]	u	142.700	4.688	−1.9131	10.989	11.55								
				5.396	−1.9186	10.983									
	^{123}Sn → ^{123}Sb			5.968	−2.3670	9.690		3.51×10^{-12}		3.96×10^{-13}		8.86×10^{0}	6.42×10^{0}		
	[0.0, $\frac{11}{2}^-$] [1337.4, $\frac{9}{2}^+$]	nu	66.200	4.688	−2.3530	9.704	9.67	3.53×10^{-12}		3.97×10^{-13}		8.88×10^{0}	6.45×10^{0}		
				5.396	−2.3627	9.694		3.53×10^{-12}		3.98×10^{-13}		8.88×10^{0}	6.46×10^{0}		
	^{123}Sn → ^{123}Sb			5.968	−3.1613	8.895		[a]		[a]		[a]	[a]		
	[0.0, $\frac{11}{2}^-$] [1337.4, $\frac{7}{2}^+$]	u	66.200	4.688	−3.1541	8.902	9.67								
				5.396	−3.1591	8.897									
	^{123}Sn → ^{123}Sb			5.968	1.8714	5.253		1.96×10^{-5}		2.82×10^{-4}		6.97×10^{-2}	1.05×10^{0}		
	[24.6, $\frac{3}{2}^+$] [160.3, $\frac{5}{2}^+$]	a	1267.900	4.688	1.8853	5.266	5.241	1.98×10^{-5}		2.88×10^{-4}		6.87×10^{-2}	1.07×10^{0}		
				5.396	1.8757	5.257		1.98×10^{-5}		2.82×10^{-4}		7.01×10^{-2}	1.05×10^{0}		
	^{123}Sn → ^{123}Sb			5.968	1.2937	7.934		2.03×10^{-8}		1.54×10^{-7}		1.32×10^{-1}	1.10×10^{0}		38.33 min
Fig. 6(e)	[24.6, $\frac{3}{2}^+$] [541.8, $\frac{3}{2}^+$]	a	886.400	4.688	1.3077	7.948	7.92	2.04×10^{-8}		1.53×10^{-7}		1.33×10^{-1}	1.10×10^{0}	40.06 min	37.45 min
				5.396	1.2981	7.939		2.04×10^{-8}		1.53×10^{-7}		1.33×10^{-1}	1.09×10^{0}		38.28 min
	^{123}Sn → ^{123}Sb			5.968	0.9597	8.110		8.93×10^{-9}		4.72×10^{-8}		1.89×10^{-1}	1.15×10^{0}		
	[24.6, $\frac{3}{2}^+$] [712.8, $\frac{1}{2}^+$]	a	715.400	4.688	0.9736	8.124	8.10	8.98×10^{-9}		4.72×10^{-8}		1.90×10^{-1}	1.15×10^{0}		
				5.396	0.9640	8.114		8.99×10^{-9}		4.72×10^{-8}		1.90×10^{-1}	1.15×10^{0}		

$^{134}Cs \rightarrow {}^{134}Ba$			6.141	0.9271	8.896		1.92×10^{-9}	7.18×10^{-9}	2.68×10^{-1}	1.22×10^{0}		
$[0.0, 4^+]$ $[1400.6, 4^+]$	a	658.100	4.832	0.9428	8.910	8.8849	1.94×10^{-9}	7.21×10^{-9}	2.70×10^{-1}	1.23×10^{0}		
			5.563	0.9372	8.905		1.92×10^{-9}	7.20×10^{-9}	2.66×10^{-1}	1.22×10^{0}		
$^{134}Cs \rightarrow {}^{134}Ba$			6.141	0.2471	9.663		1.38×10^{-10}	2.50×10^{-10}	5.51×10^{-1}	1.46×10^{0}		304.80 d
Fig. 6(f) $[0.0, 4^+]$ $[1643.3, 3^+]$	a	415.400	4.832	0.2628	9.678	9.6528	1.39×10^{-10}	2.50×10^{-10}	5.56×10^{-1}	1.46×10^{0}	2.07 yr	302.90 d
			5.563	0.2572	9.673		1.37×10^{-10}	2.50×10^{-10}	5.48×10^{-1}	1.45×10^{0}		305.56 d
$^{134}Cs \rightarrow {}^{134}Ba$			6.141	−1.8919	6.486		1.47×10^{-8}	2.14×10^{-9}	6.86×10^{0}	5.80×10^{0}		
$[0.0, 4^+]$ $[1969.9, 4^+]$	a	88.800	4.832	−1.8761	6.502	6.49	1.48×10^{-8}	2.14×10^{-9}	6.92×10^{0}	5.84×10^{0}		
			5.563	−1.8817	6.496		1.46×10^{-8}	2.14×10^{-9}	6.82×10^{0}	5.77×10^{0}		
$^{136}Cs \rightarrow {}^{136}Ba$			6.171	0.9803	7.922		1.94×10^{-8}	7.65×10^{-8}	2.53×10^{-1}	1.21×10^{0}		
$[0.0, 5^+]$ $[1866.6, 4^+]$	a	681.600	4.833	0.9960	7.938	7.91	1.95×10^{-8}	7.65×10^{-8}	2.55×10^{-1}	1.21×10^{0}		
			5.592	0.9904	7.932		1.93×10^{-8}	7.66×10^{-8}	2.51×10^{-1}	1.21×10^{0}		
$^{136}Cs \rightarrow {}^{136}Ba$			6.171	0.6625	9.718		2.10×10^{-10}	5.63×10^{-10}	3.74×10^{-1}	1.27×10^{0}		
$[0.0, 5^+]$ $[2030.5, 7^-]$	u	517.700	4.833	0.6737	9.729	$\geqslant 9.4$	2.15×10^{-10}	5.63×10^{-10}	3.81×10^{-1}	1.28×10^{0}		
			5.592	0.6697	9.725		2.11×10^{-10}	5.63×10^{-10}	3.74×10^{-1}	1.27×10^{0}		
$^{136}Cs \rightarrow {}^{136}Ba$			6.171	0.4997	7.883		1.15×10^{-8}	2.73×10^{-8}	4.20×10^{-1}	1.36×10^{0}		
$[0.0, 5^+]$ $[2053.9, 4^+]$	a	494.300	4.833	0.5155	7.899	7.87	1.16×10^{-8}	2.73×10^{-8}	4.24×10^{-1}	1.36×10^{0}		
			5.592	0.5099	7.894		1.14×10^{-8}	2.73×10^{-8}	4.18×10^{-1}	1.35×10^{0}		
$^{136}Cs \rightarrow {}^{136}Ba$			6.171	0.2202	7.255		3.40×10^{-8}	6.02×10^{-8}	5.65×10^{-1}	1.47×10^{0}		8.38 d
Fig. 7(a) $[0.0, 5^+]$ $[2140.2, 5^-]$	nu	408.000	4.833	0.2359	7.271	7.25	3.43×10^{-8}	6.02×10^{-8}	5.69×10^{-1}	1.48×10^{0}	13.16 d	8.37 d
			5.592	0.2303	7.265		3.38×10^{-8}	6.02×10^{-8}	5.62×10^{-1}	1.47×10^{0}		8.41 d
$^{136}Cs \rightarrow {}^{136}Ba$			6.171	−0.0345	6.174		2.94×10^{-7}	3.96×10^{-7}	7.42×10^{-1}	1.61×10^{0}		
$[0.0, 5^+]$ $[2207.1, 6^+]$	a	341.100	4.833	−0.0187	6.190	6.163	2.96×10^{-7}	3.96×10^{-7}	7.48×10^{-1}	1.62×10^{0}		
			5.592	−0.0243	6.184		2.93×10^{-7}	3.97×10^{-7}	7.38×10^{-1}	1.61×10^{0}		
$^{136}Cs \rightarrow {}^{136}Ba$			6.171	−0.8395	7.894		2.00×10^{-9}	1.11×10^{-9}	1.80×10^{0}	2.42×10^{0}		
$[0.0, 5^+]$ $[2356.6, 4^+]$	a	191.600	4.833	−0.8237	7.910	7.88	2.01×10^{-9}	1.10×10^{-9}	1.83×10^{0}	2.43×10^{0}		
			5.592	−0.8293	7.904		1.99×10^{-9}	1.11×10^{-9}	1.80×10^{0}	2.41×10^{0}		
$^{136}Cs \rightarrow {}^{136}Ba$			6.171	−0.9695	6.777		2.22×10^{-8}	1.07×10^{-8}	2.09×10^{0}	2.65×10^{0}		
$[0.0, 5^+]$ $[2373.7, (5)^+]$	a	174.500	4.833	−0.9537	6.792	6.768	2.25×10^{-8}	1.06×10^{-8}	2.11×10^{0}	2.66×10^{0}		
			5.592	−0.9593	6.787		2.21×10^{-8}	1.06×10^{-8}	2.08×10^{0}	2.64×10^{0}		
$^{148}Pm \rightarrow {}^{148}Sm$			6.347	3.2109	9.133		2.41×10^{-8}	8.41×10^{-7}	2.87×10^{-2}	1.04×10^{0}		
$[0.0, 1^-]$ $[0.0, 0^+]$	nu	2471.000	5.004	3.2305	9.153	9.117	2.43×10^{-8}	8.40×10^{-7}	2.90×10^{-2}	1.04×10^{0}		
			5.762	3.2170	9.139		2.43×10^{-8}	8.41×10^{-7}	2.89×10^{-2}	1.04×10^{0}		

(Continued.)

Transition details				Radius	$\log f_0t$ ($\log f_1t$) calculations			Bare atom decay rates						Half-life	
					$\log f_0$ ($\log f_1$)	$\log f_0t$ ($\log f_1t$)		λ_B (s^{-1})		λ_C (s^{-1})					
Neutral				(fm)	Present	Present	Previous	Present	Previous	Present	Previous	λ_B/λ_C	$\lambda_{Bare}/\lambda_{Neutral}$	Neutral	Bare
Atom				R_1	(for R_1)	(for R_1)		(for R_1)		(for R_1)		(for R_1)	(for R_1)		(for R_1)
Branching	Parent → daughter		Q_n	R_2	(for R_2)	(for R_2)	Ref. [4]	(for R_2)		(for R_2)		(for R_2)	(for R_2)		(for R_2)
Ref. [10]	[E (keV), J^Π]	Type	(keV)	R_3	(for R_3)	(for R_3)	Ref. [10]	(for R_3)	Ref. [4]	(for R_3)	Ref. [4]	(for R_3)	(for R_3)		(for R_3)
	^{148}Pm → ^{148}Sm			6.347	2.7716	9.467		6.81×10^{-9}		1.41×10^{-7}		4.83×10^{-2}	1.05×10^{0}		
	[0.0, 1$^-$] [550.3, 2$^+$]	nu	1920.700	5.004	2.7911	9.484	9.450	6.91×10^{-9}		1.42×10^{-7}		4.88×10^{-2}	1.06×10^{0}		
				5.762	2.7776	9.471		6.90×10^{-9}		1.42×10^{-7}		4.87×10^{-2}	1.06×10^{0}		
	^{148}Pm → ^{148}Sm			6.347	1.7677	10.061		5.31×10^{-10}		3.50×10^{-9}		1.52×10^{-1}	1.14×10^{0}		
	[0.0, 1$^-$] [1424.5, 0$^+$]	nu	1046.500	5.004	1.7872	10.080	10.048	5.37×10^{-10}		3.50×10^{-9}		1.53×10^{-1}	1.15×10^{0}		
				5.762	1.7737	10.067		5.35×10^{-10}		3.50×10^{-9}		1.53×10^{-1}	1.14×10^{0}		
	^{148}Pm → ^{148}Sm			6.347	1.7219	10.420		2.20×10^{-10}		1.38×10^{-9}		1.60×10^{-1}	1.15×10^{0}		
	[0.0, 1$^-$] [1454.2, 2$^+$]	nu	1016.800	5.004	1.7414	10.439	10.406	2.22×10^{-10}		1.38×10^{-9}		1.61×10^{-1}	1.15×10^{0}		
				5.762	1.7280	10.426		2.22×10^{-10}		1.38×10^{-9}		1.61×10^{-1}	1.15×10^{0}		
	^{148}Pm → ^{148}Sm			6.347	1.7045	7.848		8.03×10^{-8}		4.94×10^{-7}		1.63×10^{-1}	1.15×10^{0}		
	[0.0, 1$^-$] [1465.1, 1$^-$]	a	1005.900	5.004	1.7240	7.867	7.834	8.12×10^{-8}		4.95×10^{-7}		1.64×10^{-1}	1.15×10^{0}		4.92 d
				5.762	1.7105	7.854		8.10×10^{-8}		4.93×10^{-7}		1.64×10^{-1}	1.15×10^{0}	5.37 d	4.91 d
Fig. 7(b)	^{148}Pm → ^{148}Sm			6.347	1.3607	10.772		6.26×10^{-11}		2.64×10^{-10}		2.37×10^{-1}	1.21×10^{0}		4.91 d
	[0.0, 1$^-$] [1664.2, 2$^+$]	nu	806.800	5.004	1.3802	10.791	10.76	6.33×10^{-11}		2.64×10^{-10}		2.40×10^{-1}	1.22×10^{0}		
				5.762	1.3668	10.778		6.31×10^{-11}		2.64×10^{-10}		2.39×10^{-1}	1.22×10^{0}		
	^{148}Pm → ^{148}Sm			6.347	0.7812	10.307		8.82×10^{-11}		1.99×10^{-10}		4.44×10^{-1}	1.39×10^{0}		
	[0.0, 1$^-$] [1921.6, 0$^+$]	nu	549.400	5.004	0.8007	10.327	10.29	8.90×10^{-11}		1.98×10^{-10}		4.48×10^{-1}	1.39×10^{0}		
				5.762	0.7872	10.313		8.89×10^{-11}		1.99×10^{-10}		4.48×10^{-1}	1.39×10^{0}		
	^{148}Pm → ^{148}Sm			6.347	0.3652	7.898		1.33×10^{-8}		1.92×10^{-8}		6.93×10^{-1}	1.60×10^{0}		
	[0.0, 1$^-$] [2058, 2$^-$]	a	413.000	5.004	0.3848	7.918	7.885	1.34×10^{-8}		1.92×10^{-8}		7.00×10^{-1}	1.61×10^{0}		
				5.762	0.3713	7.904		1.34×10^{-8}		1.92×10^{-8}		6.98×10^{-1}	1.61×10^{0}		
	^{148}Pm → ^{148}Sm			6.347	−0.7461	7.902		3.26×10^{-9}		1.34×10^{-9}		2.44×10^{0}	3.21×10^{0}		
	[0.0, 1$^-$] [2284.4, (1, 2$^+$)]	nu	186.600	5.004	−0.7265	7.921	7.92	3.30×10^{-9}		1.34×10^{-9}		2.47×10^{0}	3.24×10^{0}		
				5.762	−0.7400	7.908		3.29×10^{-9}		1.34×10^{-9}		2.47×10^{0}	3.23×10^{0}		
	^{148}Pm → ^{148}Sm			6.347	−0.9817	8.725		3.69×10^{-10}		1.12×10^{-10}		3.29×10^{0}	3.54×10^{0}		
	[0.0, 1$^-$] [2314.0, 2$^+$]	nu	157.000	5.004	−0.9621	8.745	8.71	3.73×10^{-10}		1.12×10^{-10}		3.32×10^{0}	3.56×10^{0}		
				5.762	−0.9756	8.731		3.73×10^{-10}		1.12×10^{-10}		3.33×10^{0}	3.56×10^{0}		
	^{148}Pm → ^{148}Sm			6.347	1.7189	10.307		2.84×10^{-10}		1.77×10^{-9}		1.60×10^{-1}	1.15×10^{0}		
	[137.9, 5$^-$, 6$^-$] [1594.3, 5$^-$]	a	1014.600	5.004	1.7384	10.327	10.29	2.86×10^{-10}		1.77×10^{-9}		1.62×10^{-1}	1.15×10^{0}		
				5.762	1.7249	10.314		2.85×10^{-10}		1.77×10^{-9}		1.61×10^{-1}	1.15×10^{0}		
	^{148}Pm → ^{148}Sm			6.347	1.1505	8.362		1.24×10^{-8}		4.15×10^{-8}		2.98×10^{-1}	1.27×10^{0}		
	[137.9, 5$^-$, 6$^-$] [1905.9, 6$^+$]	nu	703.000	5.004	1.1700	8.382	8.348	1.25×10^{-8}		4.15×10^{-8}		3.01×10^{-1}	1.27×10^{0}		29.17 d
				5.762	1.1565	8.368		1.25×10^{-8}		4.15×10^{-8}		3.00×10^{-1}	1.27×10^{0}	43.23 d	29.09 d

Fig. 7(c)	^{148}Pm → ^{148}Sm		6.347	0.6821	7.963		1.72×10^{-8}	3.48×10^{-8}	4.94×10^{-1}	1.43×10^{0}	29.08 d
	[137.9, 5$^-$, 6$^-$] [2095.6, 6$^+$]	nu	513.300	5.004	0.7016	7.982	7.949	1.73×10^{-8}	3.48×10^{-8}	4.98×10^{-1}	1.43×10^{0}	
				5.762	0.6881	7.969		1.73×10^{-8}	3.48×10^{-8}	4.98×10^{-1}	1.43×10^{0}	
	^{148}Pm → ^{148}Sm			6.347	0.3723	7.192		6.82×10^{-8}	9.89×10^{-8}	6.90×10^{-1}	1.59×10^{0}	
	[137.9, 5$^-$, 6$^-$] [2194.1, 6$^+$]	nu	414.800	5.004	0.3919	7.212	7.178	6.88×10^{-8}	9.88×10^{-8}	6.97×10^{-1}	1.60×10^{0}	
				5.762	0.3784	7.198		6.88×10^{-8}	9.89×10^{-8}	6.95×10^{-1}	1.60×10^{0}	
	^{152}Eu → ^{152}Gd			6.404	2.3584	12.072		1.19×10^{-11}	1.35×10^{-10}	8.79×10^{-2}	1.10×10^{0}	
	[0.0, 3$^-$] [344.3, 2$^+$]	nu	1474.600	5.077	2.3854	12.099	12.06	1.18×10^{-11}	1.35×10^{-10}	8.74×10^{-2}	1.09×10^{0}	
				5.817	2.3710	12.085		1.18×10^{-11}	1.35×10^{-10}	8.75×10^{-2}	1.09×10^{0}	
	^{152}Eu → ^{152}Gd			6.404	1.8278	12.497		2.37×10^{-12}	1.48×10^{-11}	1.60×10^{-1}	1.16×10^{0}	
	[0.0, 3$^-$] [755.4, 4$^+$]	nu	1063.500	5.077	1.8548	12.524	12.49	2.35×10^{-12}	1.48×10^{-11}	1.59×10^{-1}	1.16×10^{0}	
				5.817	1.8404	12.509		2.36×10^{-12}	1.48×10^{-11}	1.59×10^{-1}	1.16×10^{0}	
	^{152}Eu → ^{152}Gd			6.404	1.5456	12.722		9.97×10^{-13}	4.57×10^{-12}	2.18×10^{-1}	1.21×10^{0}	
	[0.0, 3$^-$] [930.5, 2$^+$]	nu	888.400	5.077	1.5726	12.749	12.71	9.91×10^{-13}	4.57×10^{-12}	2.17×10^{-1}	1.20×10^{0}	
				5.817	1.5588	12.735		9.91×10^{-13}	4.56×10^{-12}	2.17×10^{-1}	1.20×10^{0}	
	^{152}Eu → ^{152}Gd			6.404	1.2009	12.409		1.34×10^{-12}	4.20×10^{-12}	3.18×10^{-1}	1.29×10^{0}	
	[0.0, 3$^-$] [1109.2, 2$^+$]	nu	709.700	5.077	1.2278	12.436	12.40	1.33×10^{-12}	4.20×10^{-12}	3.16×10^{-1}	1.29×10^{0}	
				5.817	1.2134	12.421		1.33×10^{-12}	4.21×10^{-12}	3.16×10^{-1}	1.29×10^{0}	
	^{152}Eu → ^{152}Gd			6.404	1.1701	10.662		7.19×10^{-11}	2.19×10^{-10}	3.28×10^{-1}	1.30×10^{0}	
	[0.0, 3$^-$] [1123.2, 3$^-$]	a	695.700	5.077	1.1970	10.689	10.654	7.15×10^{-11}	2.19×10^{-10}	3.27×10^{-1}	1.30×10^{0}	
				5.817	1.1826	10.675		7.14×10^{-11}	2.19×10^{-10}	3.27×10^{-1}	1.30×10^{0}	
	^{152}Eu → ^{152}Gd			6.404	0.7834	13.047		1.82×10^{-13}	3.65×10^{-13}	4.99×10^{-1}	1.45×10^{0}	
	[0.0, 3$^-$] [1282.2, 4$^+$]	nu	536.700	5.077	0.8104	13.074	13.04	1.81×10^{-13}	3.65×10^{-13}	4.96×10^{-1}	1.45×10^{0}	34.14 yr
				5.817	0.7960	13.060		1.81×10^{-13}	3.64×10^{-13}	4.95×10^{-1}	1.44×10^{0}	48.44 yr 34.20 yr
Fig. 7(d)	^{152}Eu → ^{152}Gd			6.404	0.6808	13.034		1.65×10^{-13}	2.95×10^{-13}	5.57×10^{-1}	1.50×10^{0}	33.99 yr
	[0.0, 3$^-$] [1318.5, 2$^+$]	nu	500.400	5.077	0.7077	13.061	13.03	1.64×10^{-13}	2.95×10^{-13}	5.54×10^{-1}	1.49×10^{0}	
				5.817	0.6933	13.046		1.64×10^{-13}	2.96×10^{-13}	5.54×10^{-1}	1.50×10^{0}	
	^{152}Eu → ^{152}Gd			6.404	0.3018	10.546		3.13×10^{-11}	3.72×10^{-11}	8.42×10^{-1}	1.73×10^{0}	
	[0.0, 3$^-$] [1434, 3$^+$]	nu	384.900	5.077	0.3288	10.573	10.537	3.11×10^{-11}	3.72×10^{-11}	8.37×10^{-1}	1.73×10^{0}	
				5.817	0.3144	10.558		3.12×10^{-11}	3.72×10^{-11}	8.37×10^{-1}	1.73×10^{0}	
	^{152}Eu → ^{152}Gd			6.404	−0.2039	11.767		9.93×10^{-13}	6.66×10^{-13}	1.49×10^{0}	2.24×10^{0}	
	[0.0, 3$^-$] [1550.2, 4$^+$]	nu	268.700	5.077	−0.1769	11.794	11.76	9.87×10^{-13}	6.66×10^{-13}	1.48×10^{0}	2.23×10^{0}	
				5.817	−0.1913	11.780		9.86×10^{-13}	6.66×10^{-13}	1.48×10^{0}	2.23×10^{0}	

(Continued.)

Transition details				Radius	$\log f_0t$ ($\log f_1t$) calculations			Bare atom decay rates						Half-life	
					$\log f_0$ ($\log f_1$)	$\log f_0t$ ($\log f_1t$)		λ_B (s^{-1})		λ_C (s^{-1})					
Neutral Atom Branching Ref. [10]	Parent → daughter [E (keV), J^Π]	Type	Q_n (keV)	(fm) R_1 R_2 R_3	Present (for R_1) (for R_2) (for R_3)	Present (for R_1) (for R_2) (for R_3)	Previous Ref. [4] Ref. [10]	Present (for R_1) (for R_2) (for R_3)	Previous Ref. [4]	Present (for R_1) (for R_2) (for R_3)	Previous Ref. [4]	λ_B/λ_C (for R_1) (for R_2) (for R_3)	$\lambda_{Bare}/\lambda_{Neutral}$ (for R_1) (for R_2) (for R_3)	Neutral	Bare (for R_1) (for R_2) (for R_3)
	^{152}Eu → ^{152}Gd			6.404	−0.5251	11.077		3.28×10^{-12}		1.51×10^{-12}		2.16×10^{0}	2.76×10^{0}		
	[0.0, 3$^-$] [1605.6, 2$^+$]	nu	213.300	5.077	−0.4981	11.104	11.07	3.25×10^{-12}		1.51×10^{-12}		2.15×10^{0}	2.75×10^{0}		
				5.817	−0.5125	11.090		3.25×10^{-12}		1.51×10^{-12}		2.15×10^{0}	2.75×10^{0}		
	^{152}Eu → ^{152}Gd			6.404	−0.7923	9.575		7.53×10^{-11}		2.51×10^{-11}		3.01×10^{0}	3.37×10^{0}		
	[0.0, 3$^-$] [1643.4, 2$^-$]	a	175.500	5.077	−0.7653	9.602	9.567	7.49×10^{-11}		2.51×10^{-11}		2.99×10^{0}	3.36×10^{0}		
				5.817	−0.7797	9.587		7.50×10^{-11}		2.51×10^{-11}		2.99×10^{0}	3.36×10^{0}		
	^{152}Eu → ^{152}Gd			6.404	−1.2313	11.100		1.35×10^{-12}		2.48×10^{-13}		5.42×10^{0}	4.94×10^{0}		
	[0.0, 3$^-$] [1692.4, 2$^+$, 3$^+$]	nu	126.500	5.077	−1.2043	11.127	11.09	1.34×10^{-12}		2.48×10^{-13}		5.40×10^{0}	4.90×10^{0}		
				5.817	−1.2187	11.112		1.34×10^{-12}		2.49×10^{-13}		5.40×10^{0}	4.91×10^{0}		
	^{152}Eu → ^{152}Gd			6.404	2.7528	7.433		8.17×10^{-7}		1.47×10^{-5}		5.57×10^{-2}	1.07×10^{0}		
	[45.5998, 0$^-$] [0.0, 0$^+$]	nu	1864.500	5.077	2.7798	7.460	7.42	8.12×10^{-7}		1.47×10^{-5}		5.54×10^{-2}	1.07×10^{0}		
				5.817	2.7654	7.455		7.95×10^{-7}		1.43×10^{-5}		5.54×10^{-2}	1.05×10^{0}		
	^{152}Eu → ^{152}Gd			6.404	3.2586	9.554		3.87×10^{-8}		3.43×10^{-7}		1.13×10^{-1}	1.09×10^{0}		
	[45.5998, 0$^-$] [344.3, 2$^+$]	u	1520.200	5.077	3.2795	9.574	9.55	3.91×10^{-8}		3.44×10^{-7}		1.14×10^{-1}	1.09×10^{0}		
				5.817	3.2683	9.563		3.88×10^{-8}		3.44×10^{-7}		1.13×10^{-1}	1.09×10^{0}		
	^{152}Eu → ^{152}Gd			6.404	1.4148	9.001		4.47×10^{-9}		1.77×10^{-8}		2.52×10^{-1}	1.23×10^{0}		
	[45.5998, 0$^-$] [1047.9, 0$^+$]	nu	816.600	5.077	1.4418	9.028	8.84	4.44×10^{-9}		1.77×10^{-8}		2.51×10^{-1}	1.23×10^{0}		
				5.817	1.4274	9.013		4.45×10^{-9}		1.77×10^{-8}		2.51×10^{-1}	1.23×10^{0}		11.72 h
Fig. 7(e)	^{152}Eu → ^{152}Gd			6.404	0.8194	7.141		1.53×10^{-7}		3.19×10^{-7}		4.81×10^{-1}	1.43×10^{0}	12.68 h	11.73 h
	[45.5998, 0$^-$] [1314.6, 1$^-$]	a	549.900	5.077	0.8464	7.168	7.13	1.52×10^{-7}		3.19×10^{-7}		4.78×10^{-1}	1.42×10^{0}		11.97 h
				5.817	0.8320	7.153		1.53×10^{-7}		3.19×10^{-7}		4.79×10^{-1}	1.43×10^{0}		
	^{152}Eu → ^{152}Gd			6.404	0.3722	8.811		1.86×10^{-9}		2.37×10^{-9}		7.82×10^{-1}	1.68×10^{0}		
	[45.5998, 0$^-$] [1460.5, 1]	nu/	404.000	5.077	0.3992	8.838	8.80	1.85×10^{-9}		2.38×10^{-9}		7.77×10^{-1}	1.67×10^{0}		
		a		5.817	0.3848	8.824		1.84×10^{-9}		2.37×10^{-9}		7.77×10^{-1}	1.67×10^{0}		
	^{152}Eu → ^{152}Gd			6.404	0.3103	8.749		[a]		[a]		[a]	[a]		
	[45.5998, 0$^-$] [1460.5, 2$^+$]	u	404.000	5.077	0.3287	8.768	8.80								
				5.817	0.3189	8.758									
	^{152}Eu → ^{152}Gd			6.404	−1.4420	6.384		5.57×10^{-8}		7.73×10^{-9}		7.21×10^{0}	6.14×10^{0}		
	[45.5998, 0$^-$] [1756.0, 1$^-$]	a	108.500	5.077	−1.4150	6.411	6.39	5.54×10^{-8}		7.53×10^{-9}		7.36×10^{0}	6.09×10^{0}		
				5.817	−1.4294	6.397		5.54×10^{-8}		7.50×10^{-9}		7.38×10^{0}	6.08×10^{0}		
	^{155}Eu → ^{155}Gd			6.446	−0.2883	8.665	8.78	1.13×10^{-9}	9.0×10^{-10}	6.88×10^{-10}	5.8×10^{-10}	1.64×10^{0}	2.35×10^{0}		
	[0.0, $\frac{5}{2}^+$] [0.0, $\frac{3}{2}^-$]	nu	252.700	5.132	−0.2613	8.692	8.65	1.12×10^{-9}		6.87×10^{-10}		1.63×10^{0}	2.34×10^{0}		
				5.857	−0.2757	8.677		1.13×10^{-9}		6.88×10^{-10}		1.65×10^{0}	2.36×10^{0}		
	^{155}Eu → ^{155}Gd			6.446	−0.6633	8.558	8.57	9.04×10^{-10}	9.2×10^{-10}	3.55×10^{-10}	3.5×10^{-10}	2.55×10^{0}	3.03×10^{0}		
	[0.0, $\frac{5}{2}^+$] [60.0, $\frac{5}{2}^-$]	nu	192.700	5.132	−0.6363	8.585	8.54	9.06×10^{-10}		3.55×10^{-10}		2.55×10^{0}	3.03×10^{0}		
				5.857	−0.6507	8.571		9.15×10^{-10}		3.54×10^{-10}		2.59×10^{0}	3.05×10^{0}		

	^{155}Eu → ^{155}Gd			6.446	−0.8657	7.912	7.91	3.17×10^{-9}	3.3×10^{-9}	9.68×10^{-10}	9.7×10^{-10}	3.28×10^{0}	3.58×10^{0}		
	$[0.0, \frac{5}{2}^+]$ $[86.5, \frac{5}{2}^+]$	a	166.200	5.132	−0.8387	7.939	7.9	3.15×10^{-9}		9.65×10^{-10}		3.26×10^{0}	3.56×10^{0}		1.31 yr
				5.857	−0.8531	7.925		3.18×10^{-9}		9.64×10^{-10}		3.30×10^{0}	3.59×10^{0}	4.75 yr	1.32 yr
Fig. 7(f)	^{155}Eu → ^{155}Gd			6.446	−1.0296	7.474	7.47	7.18×10^{-9}	7.6×10^{-9}	1.77×10^{-9}	1.8×10^{-9}	4.06×10^{0}	4.12×10^{0}		1.31 yr
	$[0.0, \frac{5}{2}^+]$ $[105.3, \frac{3}{2}^+]$	a	147.400	5.132	−1.0026	7.501	7.46	7.14×10^{-9}		1.77×10^{-9}		4.03×10^{0}	4.10×10^{0}		
				5.857	−1.0170	7.487		7.21×10^{-9}		1.76×10^{-9}		4.09×10^{0}	4.13×10^{0}		
	^{155}Eu → ^{155}Gd			6.446	−1.1471	8.750	8.73	3.31×10^{-10}	3.6×10^{-9} [b]	6.90×10^{-11}	7.2×10^{-11}	4.79×10^{0}	4.55×10^{0}		
	$[0.0, \frac{5}{2}^+]$ $[118.0, \frac{7}{2}^+]$	a	134.700	5.132	−1.1201	8.777	8.73	3.29×10^{-10}		6.83×10^{-11}		4.81×10^{0}	4.52×10^{0}		
				5.857	−1.1345	8.763		3.32×10^{-10}		6.82×10^{-11}		4.87×10^{0}	4.55×10^{0}		
	^{155}Eu → ^{155}Gd			6.446	−1.4610	8.851	8.94	1.85×10^{-10}	1.6×10^{-10}	2.44×10^{-11}	2.0×10^{-11}	7.58×10^{0}	6.21×10^{0}		
	$[0.0, \frac{5}{2}^+]$ $[146.1, \frac{7}{2}^-]$	nu	106.600	5.132	−1.4341	8.878	8.83	1.84×10^{-10}		2.48×10^{-11}		7.42×10^{0}	6.18×10^{0}		
				5.857	−1.4485	8.864		1.86×10^{-10}		2.46×10^{-11}		7.54×10^{0}	6.23×10^{0}		
	^{207}Tl → ^{207}Pb			7.099	2.6681	5.126		4.10×10^{-4}	[c]	2.53×10^{-3}	[c]	1.62×10^{-1}	1.22×10^{0}		
	$[0.0, \frac{1}{2}^+]$ $[0.0, \frac{1}{2}^-]$	nu	1418.000	5.494	2.7115	5.170	5.108	4.12×10^{-4}		2.53×10^{-3}		1.63×10^{-1}	1.22×10^{0}		
				6.484	2.6780	5.136		4.16×10^{-4}		2.53×10^{-3}		1.65×10^{-1}	1.22×10^{0}		
	^{207}Tl → ^{207}Pb			7.099	2.2681	11.123		5.08×10^{-10}		9.16×10^{-10}		5.54×10^{-1}	1.47×10^{0}		3.91 min
Fig. 8(a)	$[0.0, \frac{1}{2}^+]$ $[569.6, \frac{5}{2}^-]$	u	848.800	5.494	2.3013	11.156	>10.5	5.24×10^{-10}		9.17×10^{-10}		5.71×10^{-1}	1.49×10^{0}	4.77 min	3.92 min
				6.484	2.2756	11.131		5.18×10^{-10}		9.15×10^{-10}		5.66×10^{-1}	1.48×10^{0}		3.91 min
	^{207}Tl → ^{207}Pb			7.099	1.1450	6.169		5.83×10^{-6}		6.40×10^{-6}		9.10×10^{-1}	1.86×10^{0}		
	$[0.0, \frac{1}{2}^+]$ $[897.8, \frac{3}{2}^-]$	nu	520.200	5.494	1.1884	6.212	6.157	5.88×10^{-6}		6.41×10^{-6}		9.17×10^{-1}	1.87×10^{0}		
				6.484	1.1549	6.179		5.92×10^{-6}		6.40×10^{-6}		9.24×10^{-1}	1.88×10^{0}		
	^{228}Ra → ^{228}Ac			7.331	−2.1848	7.074		5.90×10^{-8}		5.03×10^{-11}		1.17×10^{3}	1.55×10^{2}		
	$[0.0, 0^+]$ $[6.3, 1^-]$	nu	39.500				≈7.1								
				6.707	−2.1616	7.097		5.85×10^{-8}		5.04×10^{-11}		1.16×10^{3}	1.53×10^{2}		
	^{228}Ra → ^{228}Ac			7.331	−2.1848	6.472	(6.5)	2.35×10^{-7}	2.3×10^{-7}	1.87×10^{-10}	1.8×10^{-10}	1.26×10^{3}	1.54×10^{2}		1.98 d
	$[0.0, 0^+]$ $[6.7, 1^+]$	a	39.100				≈6.5							5.75 yr	
				6.707	−2.1616	6.495		2.33×10^{-7}		1.86×10^{-10}		1.25×10^{3}	1.52×10^{2}		2.00 d
Fig. 8(b)	^{228}Ra → ^{228}Ac			7.331	−2.7515	6.206		3.50×10^{-7}		8.97×10^{-12}		3.94×10^{4}	4.58×10^{2}		
	$[0.0, 0^+]$ $[20.2, 1^-]$	nu	25.600				6.20								
				6.707	−2.7284	6.229		3.47×10^{-7}		8.96×10^{-12}		3.88×10^{4}	4.55×10^{2}		
	^{228}Ra → ^{228}Ac			7.331	−3.6585	5.123	(5.0)	3.40×10^{-6}	4.9×10^{-6}	0	0	∞	2.96×10^{3}		
	$[0.0, 0^+]$ $[33.1, 1^+]$	a	12.700				5.12								
				6.707	−3.6353	5.146		3.37×10^{-6}		0		∞	2.94×10^{3}		

(Continued.)

Transition details				Radius	$\log f_0t$ ($\log f_1t$) calculations			Bare atom decay rates						Half-life	
					$\log f_0$ ($\log f_1$)	$\log f_0t$ ($\log f_1t$)		λ_B (s^{-1})		λ_C (s^{-1})					
Neutral Atom				(fm)	Present	Present	Previous	Present	Previous	Present	Previous	λ_B/λ_C	$\lambda_{Bare}/\lambda_{Neutral}$	Neutral	Bare
				R_1	(for R_1)	(for R_1)		(for R_1)		(for R_1)		(for R_1)	(for R_1)		(for R_1)
Branching Ref. [10]	Parent → daughter $[E$ (keV), $J^\Pi]$	Type	Q_n (keV)	R_2	(for R_2)	(for R_2)	Ref. [4]	(for R_2)		(for R_2)		(for R_2)	(for R_2)		(for R_2)
				R_3	(for R_3)	(for R_3)	Ref. [10]	(for R_3)	Ref. [4]	(for R_3)	Ref. [4]	(for R_3)	(for R_3)		(for R_3)
	$^{227}Ac \rightarrow {}^{227}Th$			7.320	−1.9817	7.123	7.09	6.44×10^{-8}	7.2×10^{-8}	1.04×10^{-10}	9.8×10^{-11}	6.20×10^{2}	1.18×10^{2}		
	$[0.0, \frac{3}{2}^-]\,[0.0, (\frac{1}{2}^+)]$	nu	44.800	5.740	−1.9311	7.173	≈7.1	6.50×10^{-8}		1.04×10^{-10}		6.27×10^{2}	1.20×10^{2}		
				6.696	−1.9579	7.146		6.39×10^{-8}		1.04×10^{-10}		6.15×10^{2}	1.17×10^{2}		
	$^{227}Ac \rightarrow {}^{227}Th$			7.320	−2.3015	6.991	6.97	7.63×10^{-8}	8.3×10^{-8}	3.18×10^{-11}	2.9×10^{-11}	2.40×10^{3}	2.16×10^{2}		
	$[0.0, \frac{3}{2}^-]\,[9.3, (\frac{5}{2}^+)]$	nu	35.500	5.740	−2.2509	7.042	≈7.0	7.69×10^{-8}		3.21×10^{-11}		2.40×10^{3}	2.18×10^{2}		28.70 d
				6.696	−2.2777	7.015		7.56×10^{-8}		3.21×10^{-11}		2.42×10^{3}	2.14×10^{2}	21.93 yr	28.45 d
Fig. 8(c)	$^{227}Ac \rightarrow {}^{227}Th$			7.320	−3.0163	6.820	6.75	8.90×10^{-8}	1.1×10^{-7}	1.74×10^{-15}	0	5.11×10^{7}	8.82×10^{2}		28.95 d
	$[0.0, \frac{3}{2}^-]\,[24.5, (\frac{3}{2}^+)]$	nu	20.300	5.740	−2.9658	6.871	≈6.8	8.97×10^{-8}		1.74×10^{-15}		5.15×10^{7}	8.89×10^{2}		
				6.696	−2.9925	6.844		8.82×10^{-8}		1.74×10^{-15}		5.06×10^{7}	8.74×10^{2}		
	$^{227}Ac \rightarrow {}^{227}Th$			7.320	−4.3881	6.972		4.97×10^{-8}		0		∞	1.65×10^{4}		
	$[0.0, \frac{3}{2}^-]\,[37.9, (\frac{3}{2}^-)]$	a	6.900	5.740	−4.3376	7.022	6.9	5.02×10^{-8}		0		∞	1.66×10^{4}		
				6.696	−4.3643	6.995		4.93×10^{-8}		0		∞	1.63×10^{4}		

[a]Not calculated here; see Appendix B for details.

[b]The mismatch between λ_B value may arise from the typographical error in the tabulation of λ_B in Ref. [4].

[c]Experimentally available values are given in the section III B of the main text.

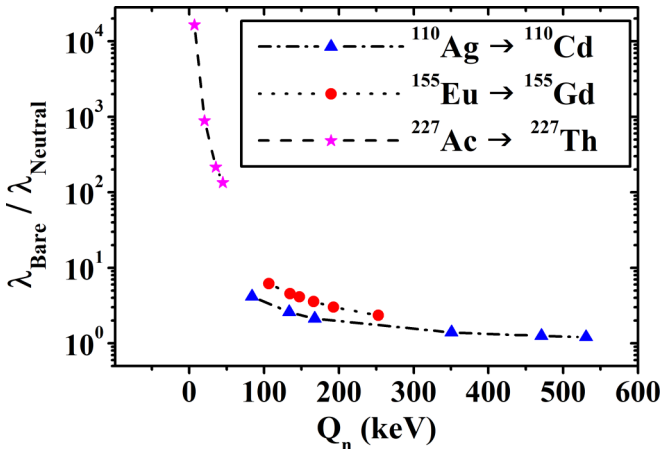

FIG. 2. Ratio of $\lambda_{\text{Bare}}/\lambda_{\text{Neutral}}$ vs the neutral-atom Q value Q_n (in keV) for various β^- transitions (for the radius R_1). See text for details.

Note that, for the β^- transition having very low Q_n value, the bound state decay may be the only path of β^- decay. As an example, in the transition of ^{227}Ac $[0.0, 3/2^-]$ to ^{227}Th $[37.9, 3/2^-]$ with $Q_n = 6.9$ keV, Q_c for continuum decay of the bare atom becomes -13.1 keV. As is evident from Eqs. (10)–(12), due to the negative value of Q_c, the corresponding decay channel gets closed. On the other hand, as $(Q_b - Q_n) > 0$ for this transition, the total decay is governed by the bound state channel only.

As an example, in Fig. 3, we have compared branchings for the neutral (left panel) and bare (right panel) ^{136}Cs atom. It can be seen from Fig. 3 that the branchings for all β^- transitions of the bare atom have been changed from that of the neutral atom. However, the ordering of each branch remains unaltered in both cases, i.e., the $[0.0, 5^+] \rightarrow [2207.1, 6^+]$ branch gets the maximum feeding followed by the $[0.0, 5^+] \rightarrow [1866.6, 4^+]$ and $[0.0, 5^+] \rightarrow [2140.2, 5^-]$ branches, whereas the minimum feed goes to the $[0.0, 5^+] \rightarrow [2030.5, 7^-]$ channel for both the neutral and bare atoms.

Furthermore, some notable observations and comments for some nuclei are given below.

(1) In the case of neutral ^{207}Tl atoms in terrestrial conditions, the $[0.0, 1/2^+]$ state of ^{207}Tl decays to the $[0.0, 1/2^-]$ state of ^{207}Pb with 99.729% branching, whereas decay to the $[569.6, 5/2^-]$ state of the daughter has the branching >0.00004% (in some places of Ref. [10] this value is given as <0.00008%) and to $[897.8, 3/2^-]$ state has 0.271% branching [10] (see Supplemental Material [21] for details). For bare atoms, Ohtsubo *et al.* [9] observed a bound state decay rate $\lambda_B = 4.29(29) \times 10^{-4}$ s^{-1} and a continuum state decay rate $\lambda_C = 2.29(012) \times 10^{-3}$ s^{-1}, by considering the transition to the $[0.0, 1/2^-]$ state of ^{207}Pb with 100% branching. In our calculation for bare atoms, we got a bound state decay rate $\lambda_B = 4.15 \times 10^{-4}$ s^{-1} and continuum state decay rate $\lambda_C = 2.54 \times 10^{-3}$ s^{-1}. The calculated branchings of bare ^{207}Tl are ≈99.6% to $[0.0, 1/2^-]$, ≈0.00005%–0.0001% to $[569.6, 5/2^-]$, and ≈0.4% to $[897.8, 3/2^-]$ states of the daughter ^{207}Pb.

In our study, we found some special cases where effective branchings for the bare atom do not follow the same ordering as that of the neutral atom. This indicates a very interesting phenomenon of branching flip, obtained for the first time in this work. Sometimes the additive contribution of λ_B and λ_C and the effect of these two competing channels can lead to this branching flip. This can be understood from Fig. 4. In Fig. 4, decay rates (s^{-1}) for neutral (λ_{Neutral}) and bare (λ_{Bare}) atom along with all decay components (λ_B and λ_C) of the bare atom versus Q_n are shown for the ground-state decay of ^{134}Cs and ^{228}Ra nuclei. One can see from Fig. 4 that the highest point corresponding to λ_{Neutral} (i.e., maximum β^- branching in neutral atoms) and the highest point corresponding to λ_{Bare} (i.e., maximum β^- branching in bare atoms) are coming from different transitions to the daughter nuclei (different Q_n values), which clearly indicates the phenomenon of flip in the branching sequence.

(2) In the case of ^{134}Cs, λ_{Neutral} is maximum at $Q_n =$ 658.1 keV, which is due to the maximum branching to the 1400.6 keV level (see Supplemental Material

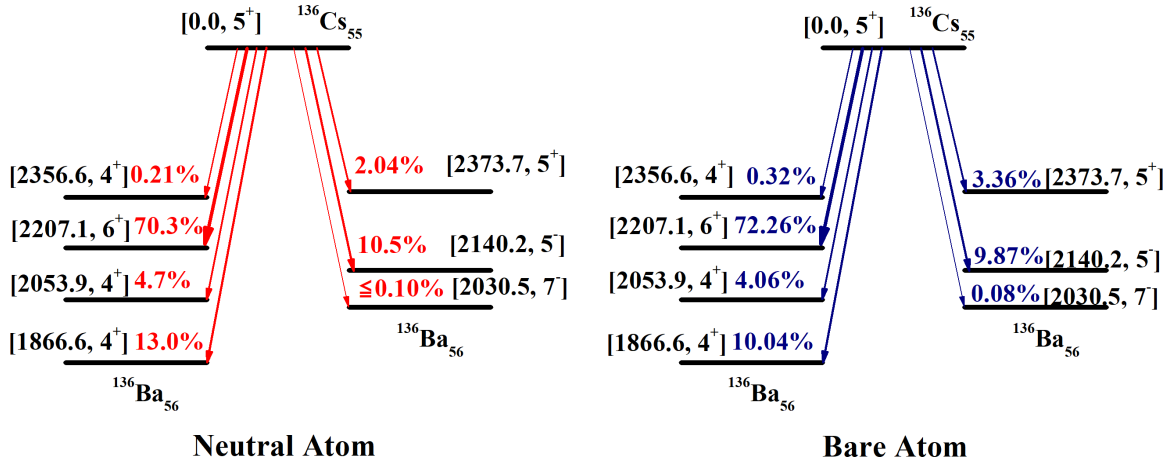

FIG. 3. Comparison of the β^--decay branchings for neutral and bare ^{136}Cs isotopes (for the radius R_1).

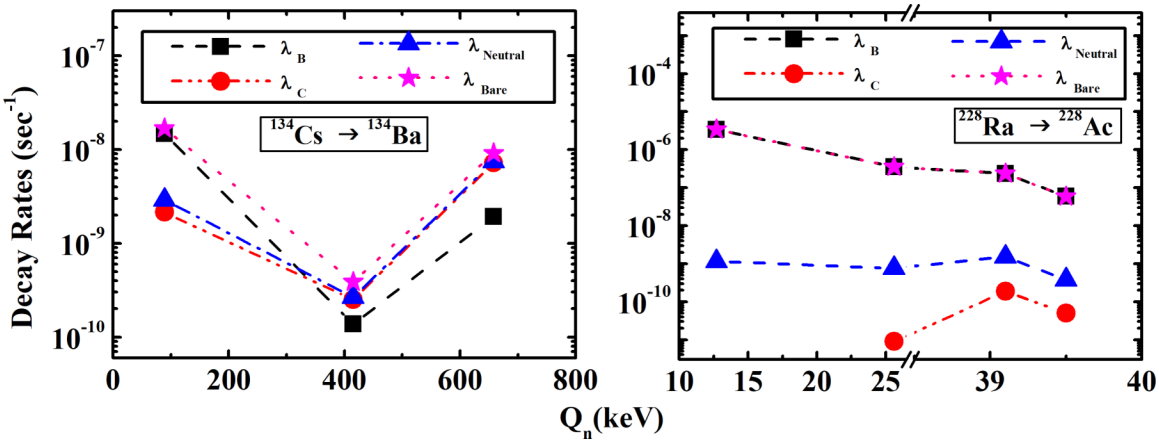

FIG. 4. Decay rates (s^{-1}) for neutral (λ_{Neutral}) and bare (λ_{Bare}) atoms along with all the decay components (λ_B and λ_C) of the bare atom (for the radius R_1) with the neutral atom Q-value Q_n (in keV). See text for details.

[21] for details) of ^{134}Ba [10]. In contrary, for the same nucleus, λ_{Bare} is maximum at $Q_n = 88.8$ keV which therefore indicates the maximum branching to the 1969.9 keV level (see Table II) of the daughter ^{134}Ba for bare atom.

(3) Similarly for ^{228}Ra, the maximum branching for the bare atom [$(\lambda_{\text{Bare}})_{\max}$ at $Q_n = 12.7$ keV] shifts from that of the neutral atom [$(\lambda_n)_{\max}$ at $Q_n = 39.1$ keV]. In Fig. 5, we have shown the change and alteration of transition branchings for the β^- decay of ^{228}Ra. One can see the branching flips of the participating levels of the ^{228}Ac atom in Figs. 4 and 5. In the case of the neutral ^{228}Ra atoms, maximum branching is 40% for the [6.7, 1$^+$] level of the daughter [10]. After complete ionization, the major contribution of the total decay rate comes due to the bound state enhancement of $Q_n = 12.7$ keV channel which has ≈84.07% decay to the [33.1, 1$^+$] level (30% in neutral atoms) of the daughter atom, whereas only ≈5.81% of the total decay branching is observed for the level [6.7, 1$^+$].

There are a few more cases where the branching flips are observed. However, not all the transition branches necessarily face the phenomenon of flip. It may also happen that only two or three branches change their sequence, whereas other branches remain in the same order as that of the neutral atom.

(4) In the β^- decay of ^{152}Eu [45.5998, 0$^-$] (see Table 1 of Ref. [21] for branching details), we find that, in both cases (neutral and bare), the branching to the [0.0, 0$^+$] branch of the daughter dominate over the rest, whereas a branching-flip is observed between [344.3, 2$^+$] and [1314.6, 1$^-$] states.

(5) Similarly for ^{227}Ac, we find that there is a branching flip between two transitions from the [0.0, 3/2$^-$] state of the parent to the [0.0, 1/2$^+$] and [24.5, 3/2$^+$] states of the daughter atom. The ratio of branching for these

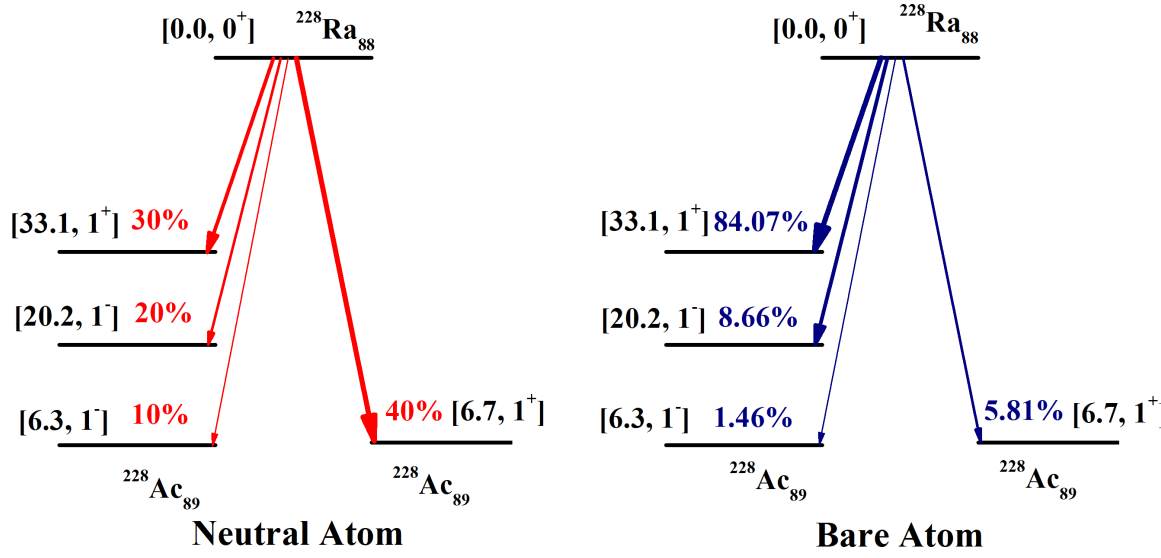

FIG. 5. Comparison of level branchings on neutral and bare ^{228}Ra isotope (for the radius R_1). Left panel shows neutral atom, right panel shows bare atom.

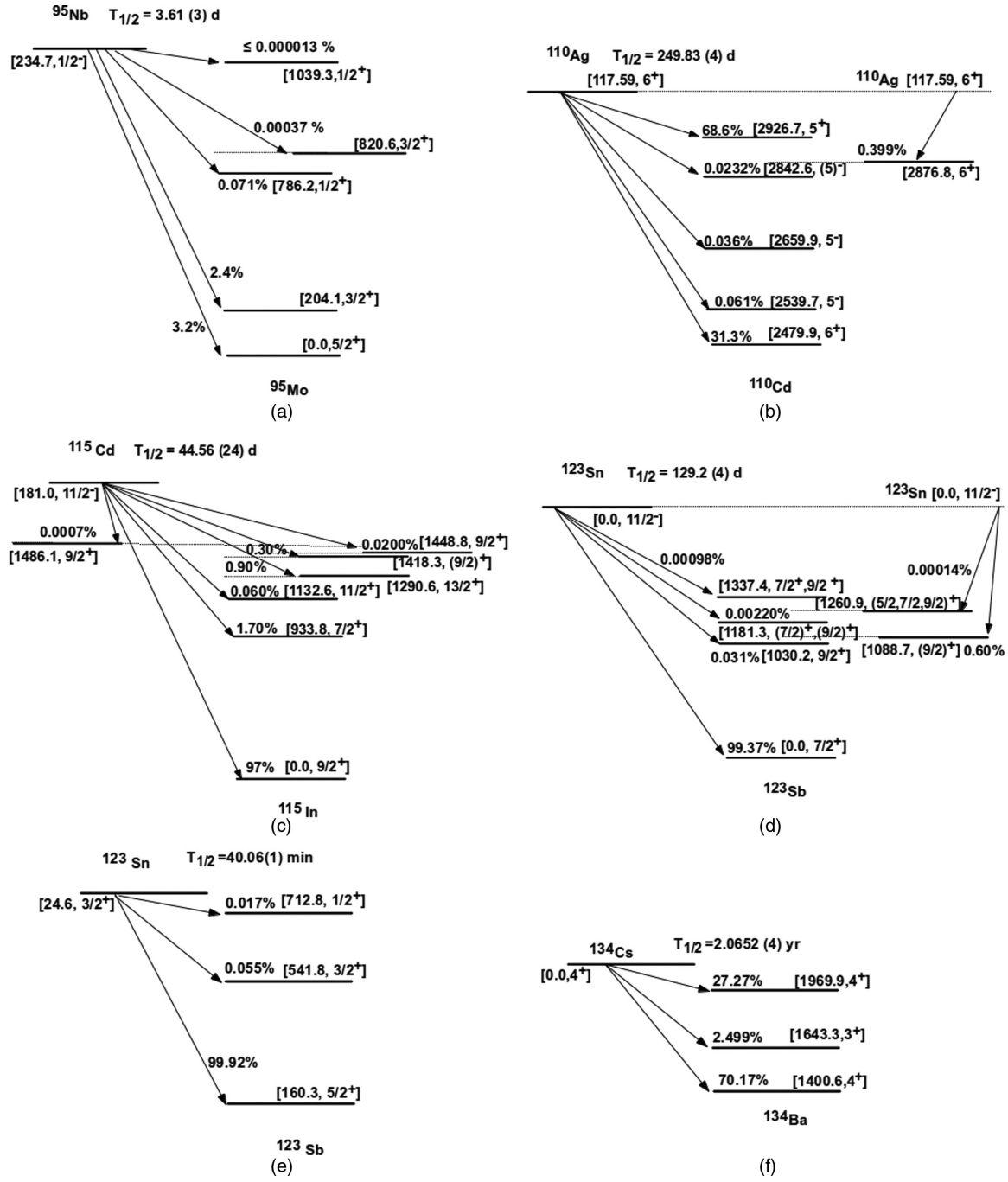

FIG. 6. β^- decay transition (^{95}Nb, ^{110}Ag, ^{115}Cd, ^{123}Sn, ^{134}Cs) with neutral atom branchings given [10]. Here, $T_{1/2}$ is the total half-life of the parent level (including all possible decay channels, viz. β, α, IT, etc.). However, only allowed (a), first-forbidden nonunique (nu), and first-forbidden unique (u) β^- decay transitions are shown in these figures.

two levels is 5.4 : 1 for neutral atoms, which changes to 1 : 1.38 for bare atoms.

Note that the ultimate fate of individual branchings in the bare atom is decided by two factors: the initial branching (required to calculate log$t$ for each transition: a part of the logft calculation) and the Q value of the neutral atom. The competition between these two factors determines whether the branching flip will occur.

2. *Effect of uncertainties*

Furthermore, to get the complete picture of β^- decay for bare atom, effects due to uncertainties in β^- decay half-life and Q value need to be considered. The effect of uncertainty is appreciable depending on the numerical value of the half-life and Q value. In case of atoms with the β^- decay half-life of the order of seconds or minutes and having high Q value, no significant change is observed in the calculation of logft due to the inclusion of experimen-

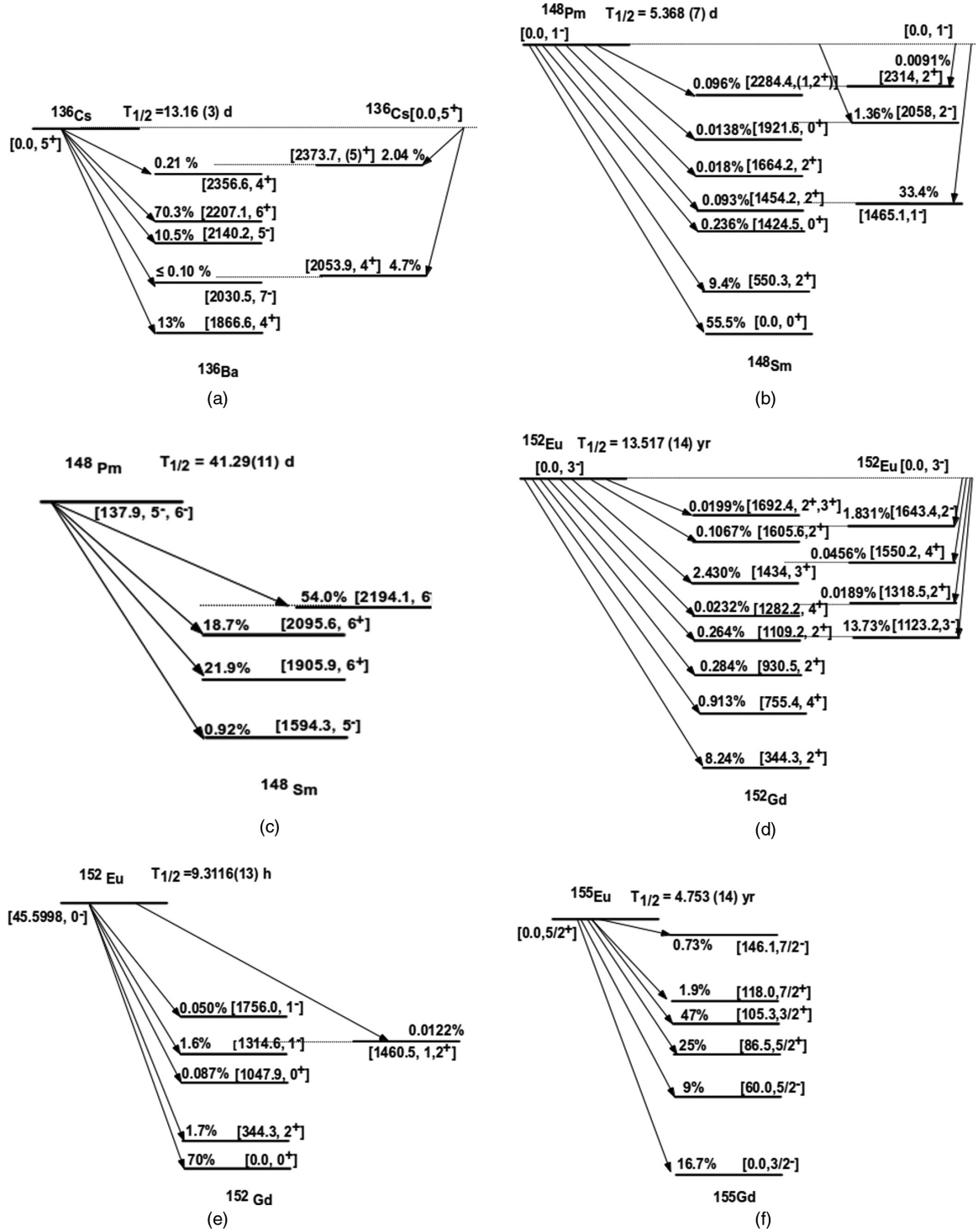

FIG. 7. β^- decay transition (^{136}Cs, ^{148}Pm, ^{152}Eu, ^{155}Eu) with neutral-atom branchings [10]. Here, $T_{1/2}$ is the total half-life of the parent level (including all possible decay channels, viz. β, α, IT, etc.). However, only allowed (a), first-forbidden nonunique (nu), and first-forbidden unique (u) β^- decay transitions are shown in these figures.

tal uncertainties. The contributions peek out for long-lived nuclei with large uncertainty or for transitions of high Q value having large uncertainty. For example, in the case of ^{93}Zr atoms, where the neutral atom half-life is equal to $1.61 \times 10^6(5)$ years, $\log ft$ for the transition $[0.0, 5/2^+ \rightarrow 30.8, 1/2^-]$ with the radius R_1 is given by $10.234^{+0.014}_{-0.013}$. Therefore, the final values for continuum and bare state β^- transitions including the uncertainties can be written as $\lambda_C = 6.87^{+0.22}_{-0.21} \times 10^{-15}$ s^{-1} and $\lambda_B = 6.13^{+0.20}_{-0.19} \times 10^{-15}$ s^{-1}, respectively.

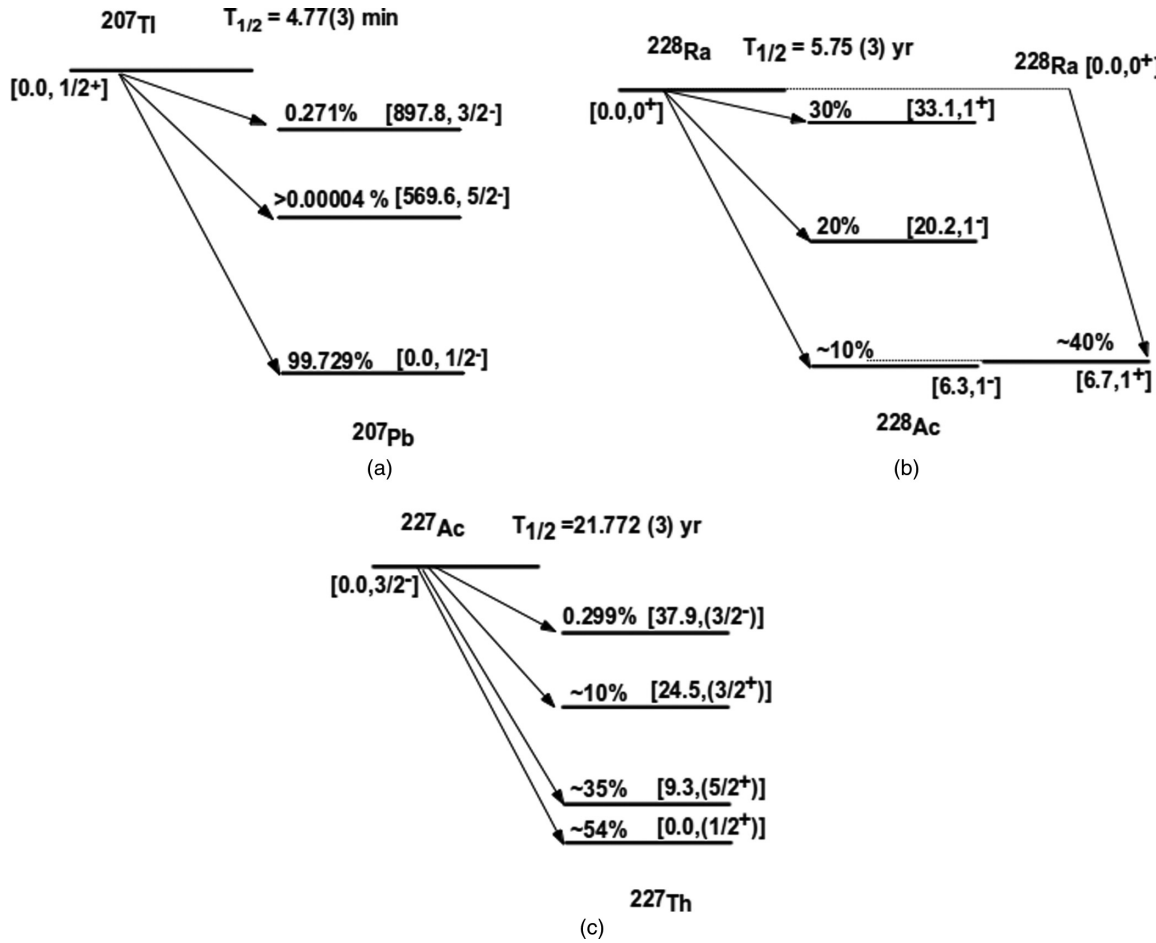

FIG. 8. β^- decay transition (^{207}Tl, ^{228}Ra, ^{227}Ac) with neutral atom branchings [10]. Here, $T_{1/2}$ is the total half-life of the parent level (including all possible decay channels, viz. β, α, IT, etc.). However, only allowed (a), first-forbidden nonunique (nu), and first-forbidden unique (u) β^- decay transitions are shown in these figures.

IV. CONCLUSION

To summarize, in this work we have calculated individual contributions of bound and continuum state β^- decays to the effective β^- decay rate of the bare atom in the $A \approx 60$ to 240 mass range where earlier information were partial and/or old.

Additionally, the dependence of transition rates over the nuclear radius and the Q value is illustrated clearly in the present study. We found a power-law dependence of λ_B/λ_C of a bare atom on Q_n for each value of Z and A. Along with the effective enhancement of transition rates, we found that transition branchings for the bare atom differs from that of the neutral atom for all Z and A, which is an outcome of nonuniform enhancement among the participating branches. Most interestingly, we have found few nuclei, viz. ^{134}Cs, ^{228}Ra, etc., where some flip in the branching pattern is found for their bare configuration. It will be interesting to see how these results help the planning of new experiments involving bare atoms. The calculations will be extended to partially ionized atoms which will provide the decay rate as function of density and temperature of the stellar plasma and will be useful for calculation of nucleosynthesis processes.

ACKNOWLEDGMENTS

A.G. is grateful to a DST-INSPIRE Fellowship (IF160297) for providing financial support. C.L. acknowledges a grant from a DST-NPDF (Grant No. PDF/2016/001348) Fellowship.

APPENDIX A: TABLE FOR β^- DECAY

Here we present a table containing $\log f_0 t (f_1 t)$ values for neutral atoms, bound and continuum state β^- decay rates for bare atoms along with the comparison with previous theoretical [4] as well as existing data [10], wherever available. Finally, a comparative study on bare atom to neutral atom β^- decay rates for different choices of radii is presented.

Explanation of table

(1) Transition details
   (a) First column: β^- decay transitions with neutral atom branchings (Figs. 6–8);
   (b) Second column: participating parent-daughter energy levels in the transition;
   (c) Third column: transition types (a, nu, and u);
   (d) Forth column: neutral atom Q value.

(2) Radii
   (a) Fifth column: R_1, R_2, and R_3 are given in consecutive rows.
(3) $\log ft$ calculations
   (a) Sixth column: $\log f_0(f_1)$ for different choices of radii (row-wise) calculated using Eqs. (2) and (5).
   (b) Seventh column: $\log f_0 t(f_1 t)$ for radii R_1, R_2, and R_3 (row-wise), where $\log ft = \log f + \log t$. Here t is the partial half-life of individual transitions (second column) calculated using $T_{1/2}$ and branching of that particular level (first column).
   (c) Eighth column: $\log f_0 t(f_1 t)$ values from previous work [4] (row 1) and existing data [10] (row 2).
(4) Bare atom decay rates
   (a) Ninth column: bound state β^- decay rates λ_B for bare atoms for different choices of radii (row-wise) calculated using Eqs. (1) and (13)–(15);
   (b) Tenth column: λ_B from previous work [4] (row 1);
   (c) Eleventh column: continuum state β^- decay rates λ_C for bare atoms for radii R_1, R_2, and R_3 (row-wise) calculated using Eqs. (1) and (10)–(12);
   (d) Twelfth column: λ_C from previous work [4] (row 1);
   (e) Thirteenth column: ratio of bound and continuum state β^- decay rates of bare atom for different choices of radii (row-wise).
(5) $\lambda_{\text{Bare}}/\lambda_{\text{Neutral}}$
   (a) Fourteenth column: ratio of bare and neutral atom decay rates for radii R_1, R_2, and R_3 (row-wise). Here, $\lambda_{\text{Bare}} = \lambda_B + \lambda_C$. λ_{Neutral} is obtained from parent level half-life ($T_{1/2}$) and β^- branching (first column).
(6) Half-life
   (a) Fifteenth column: Total β^- decay (a, nu, u) half-life of the parent level for neutral atom, obtained from $T_{1/2}$ and β^- branching (first column).
   (b) Sixteenth column: Total β^- decay (a, nu, u) half-life of the parent level for bare atom for radii R_1, R_2, and R_3 (row-wise). It is obtained by the formula $0.693 \times 1/\sum_i(\lambda_{\text{Bare}})_i$, where i denotes all the possible a, nu, and u type of β^- transitions. Here, min = minutes; h = hours; d = days; yr = years.

APPENDIX B: CHOICE OF SPIN-PARITY FOR UNCONFIRMED STATES OF NEUTRAL ATOM

Sometimes the comparison of the calculated $\log ft$ values with experimental data gives an idea about the spin-parity of participating energy levels where these quantities are still unconfirmed experimentally. We have identified a few such transitions in Table II. In the transition from ^{123}Sn [0.0, $11/2^-$], there are a few states of the daughter ^{123}Sb, where the spin values are not experimentally confirmed yet [identified as $(J)^\pi$ and/or (J^π) in the table]. In the transition from ^{123}Sn [0.0, $11/2^-$] to $E = 1181.3$ keV state of the daughter, if it chooses the decay channel with the spin-parity $J^\pi = (9/2)^+$ then the transition will be of the type (nu), whereas for the choice of spin $J^\pi = (7/2)^+$, the transition [0.0, $11/2^- \rightarrow$ 1181.3, $(7/2)^+$] will be the (u) type. Now comparing with the available experimental $\log ft$ value, it seems from our calculation that the (nu) case is in good agreement whereas the (u) case deviates (difference $\approx$0.4) from the same for all choices of the radius R.

Similarly, from Table II, our observations for other such transitions are given by (see the table for $\log ft$ comparison)

(1) ^{123}Sn [0.0, $11/2^-$] $\rightarrow$ ^{123}Sb [1260.9, $(9/2)^+$]: (nu);
(2) ^{123}Sn [0.0, $11/2^-$] $\rightarrow$ ^{123}Sb [1337.4, $9/2^+$]: (nu);
(3) ^{152}Eu [45.5998, 0^-] $\rightarrow$ ^{152}Gd [1460.5, 1^+]: (nu).

Note 1. This type of study is not conclusive in the transition from [137.9, 5^-, 6^-] level of the ^{148}Pm nucleus. Depending on the spin of the parent level $5^-/6^-$, all four transitions to the daughter level will either be of type (a) or of type (nu) and thus the $\log ft$ value in each case will remain the same.

Note 2. In case of the ^{152}Eu [45.5998, 0^-] to ^{152}Gd [1047.9, 0^+] transition our $\log ft$ differs from that of the experimental value [10] by a difference of $\approx$0.16–0.18 (for different radii). However, we find a numerical mismatch in the tabulation for the experimental energy value of [1047.9, 0^+] state of ^{152}Gd [10,23].

Note 3. For the β^- transitions from the first-excited state of ^{95}Nb, the parent level is mentioned as [234.7, $1/2^-$] in Ref. [24], whereas in Ref. [10] this energy level is mentioned both as [235.7, $1/2^-$] and [234.7, $1/2^-$] at different places. However, our calculation of $\log ft$ matches with the reported $\log ft$ value only when we have taken the level energy as 234.7 keV.

[1] R. Daudel, M. Jean, and M. Lecoin, J. Phys. Radium **8**, 238 (1947).
[2] J. N. Bahcall, Phys. Rev. **124**, 495 (1961).
[3] K. Takahashi and K. Yokoi, At. Data Nucl. Data Tables **36**, 375 (1987).
[4] K. Takahashi, R. N. Boyd, G. J. Mathews, and K. Yokoi, Phys. Rev. C **36**, 1522 (1987).
[5] K. Takahashi and K. Yokoi, Nucl. Phys. A **404**, 578 (1983).
[6] M. Jung *et al.*, Phys. Rev. Lett. **69**, 2164 (1992).
[7] F. Bosch *et al.*, Phys. Rev. Lett. **77**, 5190 (1996).
[8] K. Yokoi, K. Takahashi, and M. Arnould, Astron. Astrophys. **117**, 65 (1983).
[9] T. Ohtsubo *et al.*, Phys. Rev. Lett. **95**, 052501 (2005).
[10] National Nuclear Data Center, https://www.nndc.bnl.gov/.
[11] N. B. Gove and M. J. Martin, At. Data Nucl. Data Tables **10**, 205 (1971).
[12] E. J. Konopinski and G. E. Uhlenbeck, Phys. Rev. **60**, 308 (1941).

[13] H. Behrens and J. Jänecke, *Numerical Tables for Beta-Decay and Electron Capture* (Springer-Verlag, Berlin, Heidelberg, 1969).
[14] J. N. Bahcall, Phys. Rev. **129**, 2683 (1963).
[15] B. Budick, Phys. Rev. Lett. **51**, 1034 (1983).
[16] W. R. Garrett and C. P. Bhalla, Eur. Phys. J. A **198**, 453 (1967).
[17] L. Hayen, N. Severijns, K. Bodek, D. Rozpedzik, and X. Mougeot, Rev. Mod. Phys. **90**, 015008 (2018).
[18] Atomic Spectra Database, https://physics.nist.gov/PhysRefData/ASD/ionEnergy.html.
[19] A. C. Hayes, J. L. Friar, G. T. Garvey, Gerard Jungman, and G. Jonkmans, Phys. Rev. Lett. **112**, 202501 (2014).
[20] F. Salvat, J. M. Fernandez-Varea, and W. Williamson, Jr., Comput. Phys. Commun. **90**, 151 (1995).
[21] See Supplemental Material at http://link.aps.org/supplemental/10.1103/PhysRevC.100.064313 for the complete dataset.
[22] I. Angeli and K. P. Marinova, At. Data Nucl. Data Tables **99**, 69 (2013).
[23] M. J. Martin, Nucl. Data Sheets **114**, 1497 (2013).
[24] S. K. Basu, G. Mukherjee, and A. A. Sonzogni, Nucl. Data Sheets **111**, 2555 (2010).